Nanoscale

ROYAL SOCIETY OF CHEMISTRY

REVIEW

View Article Online
View Journal | View Issue

Cite this: *Nanoscale*, 2024, **16**, 3269

Nanochitin for sustainable and advanced manufacturing

Pei Lin Chee,[a,b] Thenapakiam Sathasivam,[b] Ying Chuan Tan,[b] Wenya Wu,[a] Yihao Leow,[a] Quentin Ray Tjieh Lim,[a,c] Pek Yin Michelle Yew,[a,b] Qiang Zhu[a,d] and Dan Kai*[a,b,d]

Received 1st November 2023,
Accepted 11th January 2024

DOI: 10.1039/d3nr05533g

rsc.li/nanoscale

Presently, the rapid depletion of resources and drastic climate change highlight the importance of sustainable development. In this case, nanochitin derived from chitin, the second most abundant renewable polymer in the world, possesses numerous advantages, including toughness, easy processability and biodegradability. Furthermore, it exhibits better dispersibility in various solvents and higher reactivity than chitin owing to its increased surface area to volume ratio. Additionally, it is the only natural polysaccharide that contains nitrogen. Therefore, it is valuable to further develop this innovative technology. This review summarizes the recent developments in nanochitin and specifically identifies sustainable strategies for its preparation. Additionally, the different biomass sources that can be exploited for the extraction of nanochitin are highlighted. More importantly, the life cycle assessment of nanochitin preparation is discussed, followed by its applications in advanced manufacturing and perspectives on the valorization of chitin waste.

[a]*Institute of Materials Research and Engineering (IMRE), Agency for Science, Technology and Research (A*STAR), 2 Fusionopolis Way, Innovis #08-03, 138634, Singapore. E-mail: kaid@imre.a-star.edu.sg*
[b]*Institute of Sustainability for Chemicals, Energy and Environment (ISCE²), Agency for Science, Technology and Research (A*STAR), 2 Fusionopolis Way, Innovis #08-03, 138634, Singapore*
[c]*Department of Materials Science and Engineering, National University of Singapore, 9 Engineering Drive 1, 117576, Singapore*
[d]*School of Chemistry, Chemical Engineering and Biotechnology, Nanyang Technological University, 62 Nanyang Dr, Singapore 637459*

1 Introduction

The generation of 6–8 million tons of crustacean waste annually[1] presents an issue of inefficient resource utilization where instead of being exploited to produce value-added products, these valuable resources are discarded, contributing to the problem of waste accumulation. This increasing accumulation of waste does not conform to the expected trend of sus-

Pei Lin Chee

*Ms Pei Lin Chee obtained her Bachelor's of Engineering in Biomedical Engineering (2014) and Master's of Engineering in Materials Science and Engineering (2019) from the National University of Singapore (NUS). She is presently working at the Institute of Sustainability for Chemicals, Energy and Environment (ISCE2), A*STAR, Singapore. Her research interests are focused on the area of converting waste materials into functional materials such as coatings and bioinks.*

Dan Kai

*Dr Dan Kai obtained his PhD from the NUS Graduate School for Integrated Science & Engineering, National University of Singapore. Currently, he is working as a Principal Scientist and Group Leader at the Institute of Materials Research and Engineering & Institute of Sustainability for Chemicals, Energy and Environment, A*STAR, Singapore. His research interests are focused on the synthesis of biomass-based functional materials (including nanoparticles, polymers, hydrogels and nanofibers) for high-performance green composites and healthcare biomaterials. He is also interested in the valorization of argi-food waste for value-added applications.*

tainability. Thus, to achieve the goals of sustainability and circular economy and considering the advantages of chitin, research efforts have been devoted to its valorization.

The discovery of chitin dates back to 1811. Subsequently, after more than a century of investigation and exploration, various approaches have been developed to extract/process chitin on different scales, and thus it can be employed in various applications (Fig. 1a). As a linear polysaccharide composed of β(1 → 4)-linked 2-acetoamido-2-deoxy-β-D-glucose units, chitin is the second most abundant renewable biopolymer in the world after cellulose. Moreover, chitin can be further classified as α, β and γ depending on the alignment of its molecular chains.[2] In α-chitin, molecular chains are arranged in an antiparallel fashion, whereas β-chitin has parallel molecular chains.[2] Alternatively, γ-chitin is made up of both parallel and antiparallel molecular chains. Among them, α-chitin is the most stable form and it exists as the backbone of the exoskeleton of crustaceans and insects and in the cell walls of microorganisms.[2] In contrast, β-chitin can be found in squid pen, tubeworms, and cuttlefish bone,[2] while γ-chitin is found in some cocoons and mushrooms.[3] Thus, chitin has attracted interest from researchers not just because it is abundant and affordable, but also because it can impart toughness and resistance to materials.[1] Furthermore, by adjusting its concentration, the toughness and resistance of the corresponding materials can be varied and closely regulated to achieve the intended purpose. Furthermore, chitin has many other attractive benefits such as biodegradability, low allergenicity, biocompatibility and easy processability.[1]

Nanochitin is structurally made up of a bundle of semicrystalline chitin nanofibrils that are held together by van der Waals forces and hydrogen bonding.[1] It usually exists together with protein and minerals. Hence, deproteinization and demineralization are necessary to isolate nanochitin. To date, researchers have explored various forms of nanochitin, such as nanocrystals and nanofibers.[4] By breaking down chitin to nanoscale dimensions, the reactivity of the chitin can be preserved, while its solubility/dispersibility can be improved,[1,5] thereby extending its applications. Nanochitin is an attractive polymer given that it is the only natural polysaccharide that contains nitrogen, which can serve as a natural nitrogen source to produce nitrogen-containing chemicals, *e.g.* compounds used in pharmaceuticals.[6] Also, as an elemental building block of chitin, nanochitin possesses the advantages of chitin such as toughness, easy processability and biodegradable. Additionally, the presence of acetamide groups on the nanochitin endows it with antimicrobial activities, non-toxicity and wound-healing ability.[3] However, although there are an increasing number of publications on nanochitin annually, it research still lags behind its parent chitin (Fig. 1b). The increasing attention on nanochitin is illustrated by its increasing number of citations, as shown in Fig. 1c.

This review aims to provide readers with knowledge on the various methods to synthesize nanochitin. Generally, these

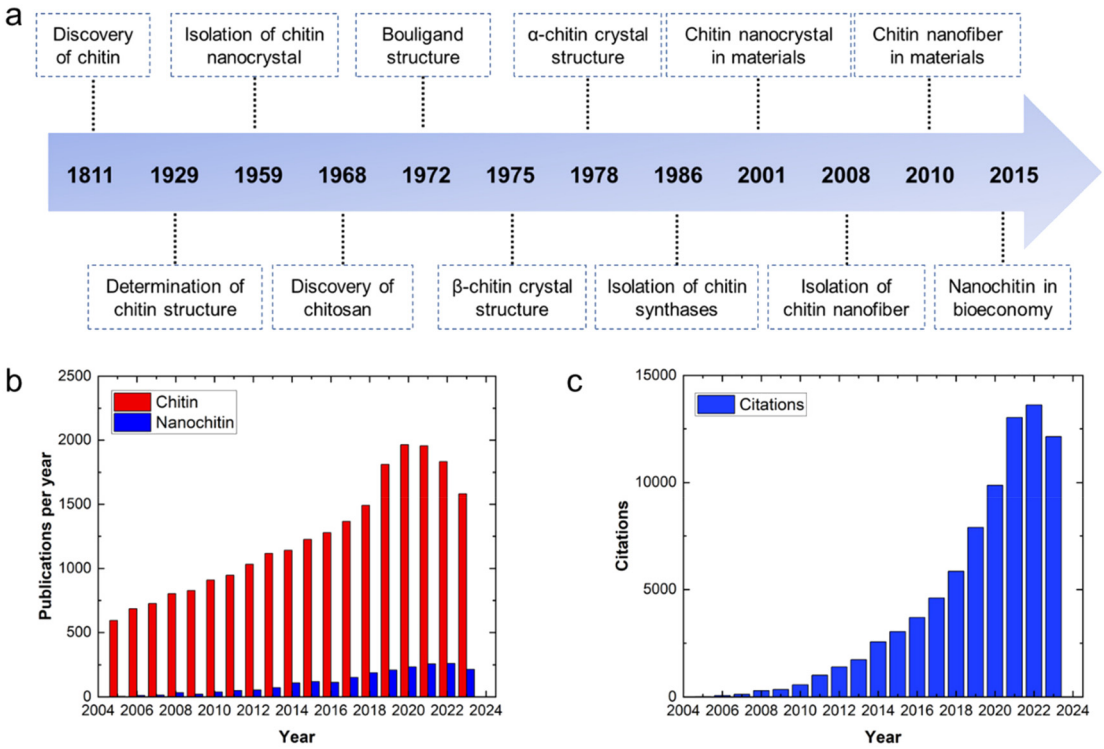

Fig. 1 (a) Timeline of chitin and nanochitin from their discovery to analysis and applications. Adapted with permission.[1] Copyright 2022, the American Chemical Society. (b) Annual publications on chitin and nanochitin from 2005 to 2023. (c) Annual citations on nanochitin from 2005 to 2023. The data was obtained from the Web of Science, 14th December 2023.

methods are categorized as chemical and mechanical treatments. In contrast, we summarize the recent approaches in a new light by further grouping them into traditional and sustainable approaches to aid researchers to push the frontier of sustainable research. Furthermore, the different sources of biomass that can be exploited for the extraction of chitin are highlighted. Although the valorization of crustacean waste, specifically chitin, into value-added products is desirable to achieve a circular economy, its environmental impact from cradle to grave needs to be determined, which is attempted herein by life cycle assessments to present the true benefits of its valorization. Finally, this review is concluded with the potential range of applications of nanochitin in such as in the field of 3D printing, photonics, packaging and catalysis, followed by a perspective on the sustainable use of nanochitin.

2 Biomass sources for chitin

Chitin is traditionally sourced from the seafood industry, where the exoskeletons of crustaceans such as shrimps, crabs and crawfish are discarded as waste.[7] Alternatively, to diversify the future sources of chitin, other forms of supplies are also studied. In general, chitin exists in three types of polymorphs (Fig. 2), where α-chitin is the main isomorph present in the exoskeletons of crustaceans and molluscs, β-chitin is found in squid pens, while γ-chitin exists in the cocoon fibers of *Ptinus* beetles.[4] These polymorphs differ in the stacking arrangement of the polymeric chitin chains. Due to this difference, the degree of H-bonding interactions from the amide functional groups between the polymeric chains differ, and thus exhibit different properties. In particular, α-chitin and β-chitin contain polymeric chitin chains that are stacked in anti-parallel and parallel configurations, respectively. Alternatively, γ-chitin consists of both anti-parallel and parallel arrangements of chitin chains. Generally, chitin has been extracted and studied from three groups of sources, *i.e.*, aquatic invertebrates, insects, and fungi.[8] Generally, the extraction process involves demineralization (acid treatment), deproteinization (alkaline treatment) and decolorization steps. Furthermore, all these treatments need to be optimized according to the chitin source due to the differences in physicochemical properties.

2.1 Aquatic invertebrates

Aquatic invertebrates, such as crustaceans, molluscs and cephalopods, represent an important food source globally. In particular, the exoskeletons of crustaceans, which are also major waste products in the seafood industry, have been exten-

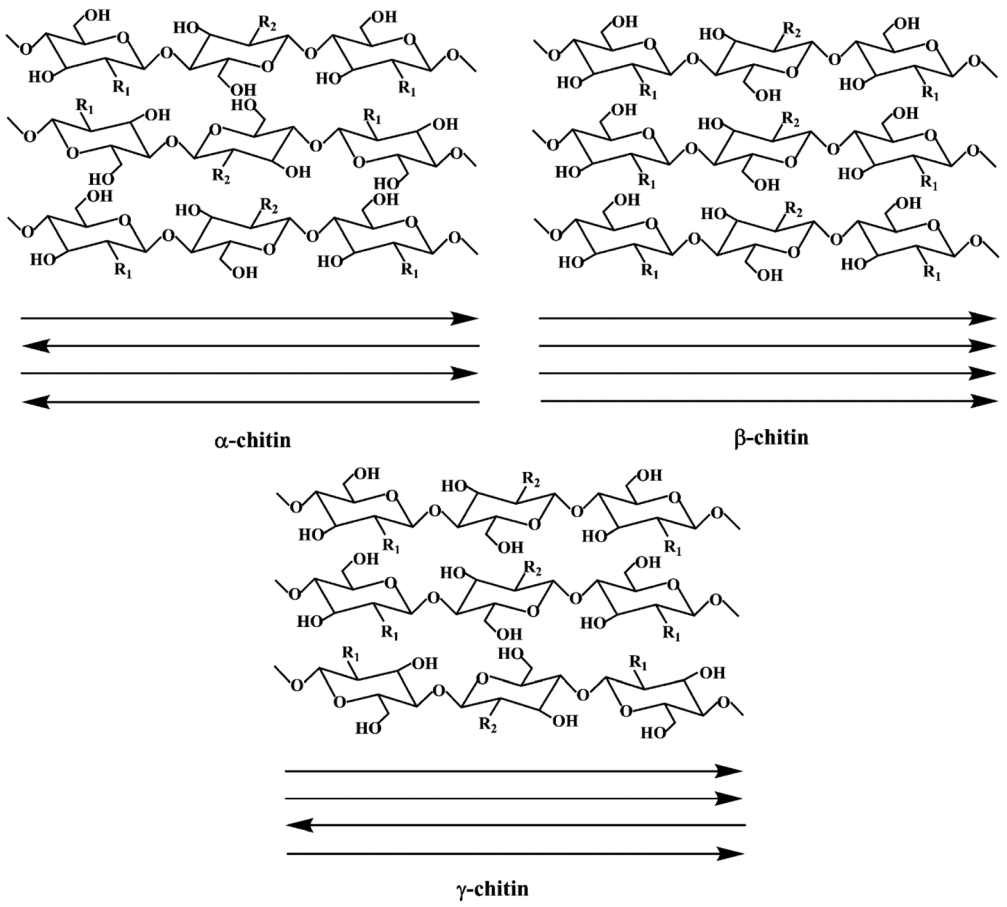

Fig. 2 Schematic illustration of the three types of chitin polymorphs. Reproduced with permission.[9] Copyright 2020, John Wiley and Sons.

sively studied as a source of chitin.[10] Presently, they are the primary sources of commercially produced chitin.[7] More specifically, shrimp shells are more commonly used as the source of chitin due to their thinner exoskeleton, making the extraction of chitin easier than other forms of shells. Generally, crustacean shells are harder and more brittle than the other chitin sources due to the well-connected network among chitin, minerals and proteins. Therefore, the chitin extraction process is harsher, which requires crushing and concentrated acids for adequate demineralization. Alternatively, milder chemical or enzymatic treatments have also been proposed, although this approach is still not widely adopted in industry. Generally, crustacean shells are comprised of chitin (20–30%), proteins (30–40%), inorganic minerals (30–60%), and lipids (0–14%).[11] Furthermore, these compositions vary significantly across species and seasons.

Rajeevgandhi and team studied the extraction of chitin from various crustacean shells, *i.e.* crab, lobster, shrimp and squilla.[12] Utilizing the traditional chemical treatments for chitin extraction, the chitin yields from the four types of crustaceans were 21.25%, 17.50%, 20.00% and 23.75%, respectively. As presented in Fig. 3a, the surface morphologies of the extracted chitin differed among the sources. The shrimp and crab chitins exhibited porous structures at low magnifications and nanofibrous structures at high magnifications. The squilla chitin showed the opposite characteristics, while lobster chitin mainly displayed nanofibrous structures. Considering that the surface structures can affect the potential functionalities of nanochitin, it is important to choose the appropriate chitin source. The authors also found that the chitin obtained from this work has a low molecular weight, which is classified as below 50 kDa. In general, chitin with low molecular weight is desirable for chemo-drug delivery applications.

2.2 Insects

There has been an increasing number of industrial farms that produce insects as a new source of protein for feed and food.[13] Thus, considering that insects contain chitin, insect farms can be a potential continuous source of chitin. Furthermore, the exoskeletons of insects contain less inorganic minerals than the shells of crustaceans, and thus the yield of chitin can be potentially higher, while the chitin extraction process milder.

Huet and colleagues investigated the extraction of chitin from *Bombyx eri* larvae.[14] The authors highlighted that the chitin contents in the cuticles of the larvae and the shells of shrimps were 45% and 19%, respectively. Furthermore, the mineral content in the studied insect chitin was significantly lower than that in shrimp chitin (1.9% *vs.* 21.7%). Therefore, it is theoretically possible to achieve a higher chitin yield and milder extraction process from this insect source. The authors demonstrated this by obtaining a chitin yield of 31.1% with a purity of 89.9% *via* a single-step extraction process without demineralization. With the same extraction process applied to shrimp shells, the chitin yield was 17.1% with a purity of less than 65.0%.

Black soldier flies (BSFs), *Hermetia illucens*, are one of the most studied insects as feed. This is largely due to the ability of this species to thrive on various organic streams, especially manure and food wastes. In addition, the byproducts formed at various lifecycle stages of the insects contain chitin. Soetemans *et al.* studied the extracted chitin at different stages of the lifecycle of BSFs, namely, the larvae, sheddings, prepupae, pupae, cocoons and flies (Fig. 3b).[15] All these chitin samples were found to be mainly composed of α-chitin, similar to shrimp chitin. Among them, the sheddings were the most difficult to purify (75.7%) even though they exhibited one of the highest chitin contents. This can be attributed to their higher mineral content, which requires a harsher extraction process. Alternatively, the cocoons of BSFs were identified to possess a high chitin content of 24% and the extracted chitin exhibited a crystallinity index and purity of 94% and 97%, respectively. Nonetheless, the authors concluded that the various chitin samples generally had minor differences in their physicochemical properties, and thus it is still possible to perform a convenient homogeneous chitin extraction process with all chitin-containing byproducts simultaneously.

2.3 Fungi

Chitin is also present as the major polymeric component in the cell wall of certain groups of fungi, *e.g.*, Ascomycetes, Basidiomycetes, Deuteromycetes, and Zygomycetes.[8] In fact, chitin was first isolated from a fungus source by Braconnot in the early 1800s. Although fungi generally contain a lower chitin content compared to crustaceans (10–26%), fungi chitin is attracting increasing academic and commercial attention. This is because fungal-based chitin is advantageous compared to animal-based chitin due to its absence of inorganic minerals, more uniform composition, abundant non-seasonal availability and vegan source.[18] However, the chitin in fungi exists as a component of a network with other polysaccharides, *e.g.*, cellulose, mannan, and glucan, thus complicating the chitin extraction process. Specifically, chitin and β-glucan are connected *via* covalent bonds. Therefore, a chitin-β-glucan complex is commonly obtained after performing the alkaline treatment on fungi sources (without demineralization step). Thus, to obtain pure chitin from this complex, acid treatments are required to selectively degrade the glucan components.[19]

Due to the species-richness of fungi, it can be expected that the properties of the extracted chitin will vary considerably. Vetter investigated the chitin content of various cultivated edible mushrooms (*Agaricus bisporus*, *Pleurotus ostreatus* and *Lentinula edodes*).[20] Among them, the saprotrophic *A. bisporus* contained the highest chitin composition of 6.7–8.8% (other two: 2.2–8.1%). Bamba *et al.* showed that α-chitin nanofibrils from the microalgae *Phaeocystis globosa* had comparable tensile strength as that extracted from squid pens and tubeworms.[21] Considering the large amount of spent biomass produced during fermentation, such as the production of citric acid, studies have also been conducted to investigate the chitin content of *Aspergillus niger*.[22] The yield of the extracted chitin-β-glucan complex was 44% with a good chitosan content of more than 32% (Table 1).

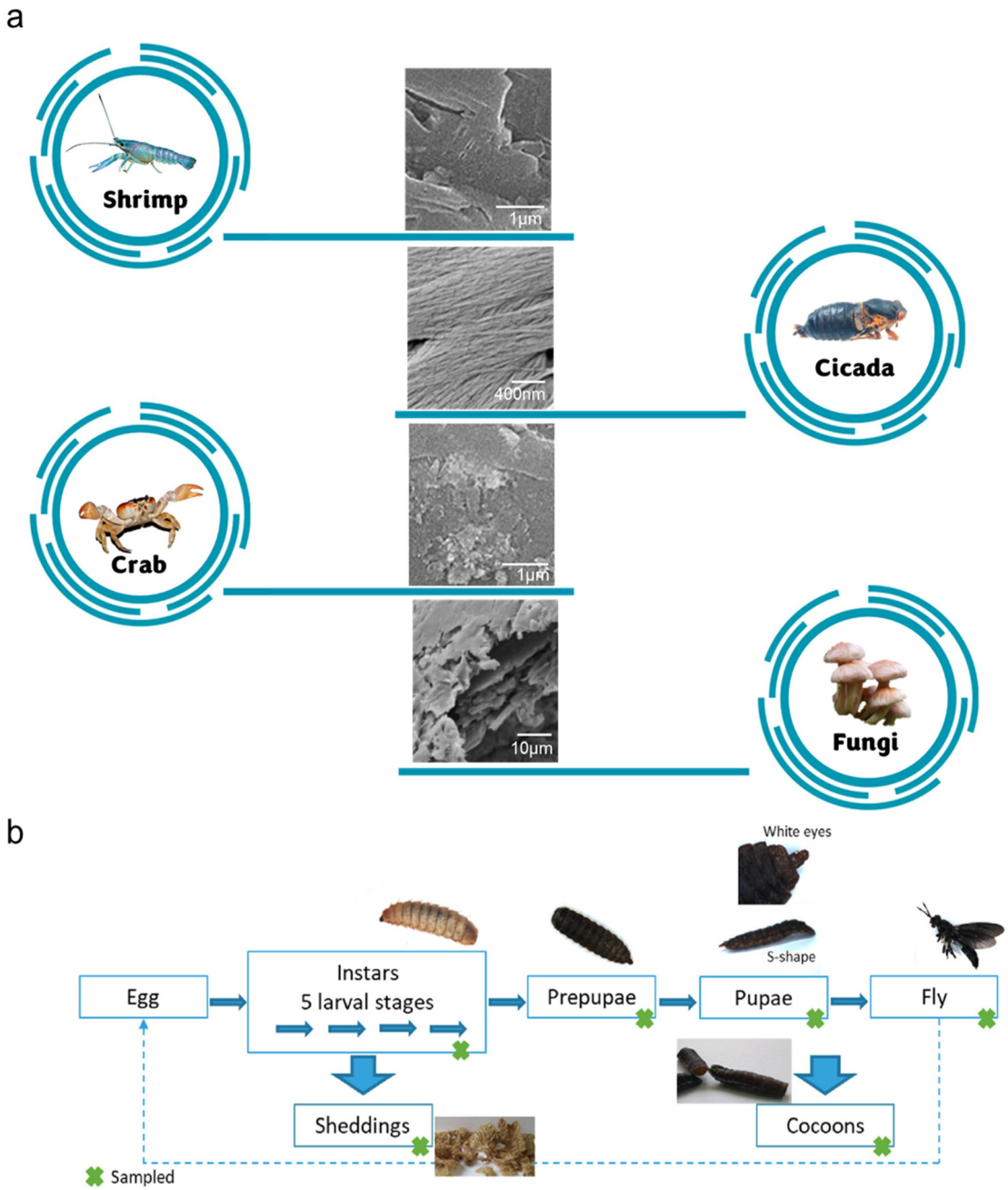

Fig. 3 (a) SEM images of chitin from various sources. Adapted with permission.[12] Copyright 2021, Elsevier Ltd.[16] Copyright 2016, Elsevier Ltd.[17] Copyright 2023, Elsevier B.V. (b) Investigation of chitin extraction from various life stages of BSF. Reproduced with permission.[15] Copyright 2020, Elsevier Ltd.

3 Nanochitin fabrication

The preparation of nanochitin usually involves two main steps. It starts with the purification step of chitin, which primarily involves (i) deproteinization using alkali or enzyme hydrolysis, (ii) demineralization achieved by using acid and (iii) removal of lipids and pigment *via* bleaching treatment. Then, the purified chitin can be attained in either the dry or wet state for further processing.[23,24] The subsequent step to attain nanochitin (*i.e.*, nanocrystals and nanofibers) is comprised of the microfabrication of the purified chitin and the various methods to achieve it can be categorized into either the traditional approach or sustainable approach. Fig. 4 illustrates the various methods for the preparation of nanochitin.

3.1 Traditional approach

The use of chemicals, mechanical disintegration, electrospinning, wet spinning and self-assembly methods to obtain

Table 1 Summary of selected examples of chitin sources

Source	Chitin yield (%)	Properties	Ref.
Crab (shells)	21.3	Porous, nanofibrous	12
Lobster (shells)	17.5	Nanofibrous	12
Shrimp (shells)	20.0	Porous, nanofibrous	12
Squilla (shells)	23.8	Nanoporous, fibrous	12
Bombyx eri larvae (cuticles)	31.1	No demineralization required	14
Black soldier flies (cocoons)	24.0	High crystallinity and purity	15
Mushroom *A. bisporus*	6.7–8.8	Higher chitin level in the pileus (cap)	20
Microalgae *Phaeocystis globosa*	—	Nanofibrils with high tensile strength	21
Aspergillus niger	44.0%	Exists as chitin-β-glucan complex	22

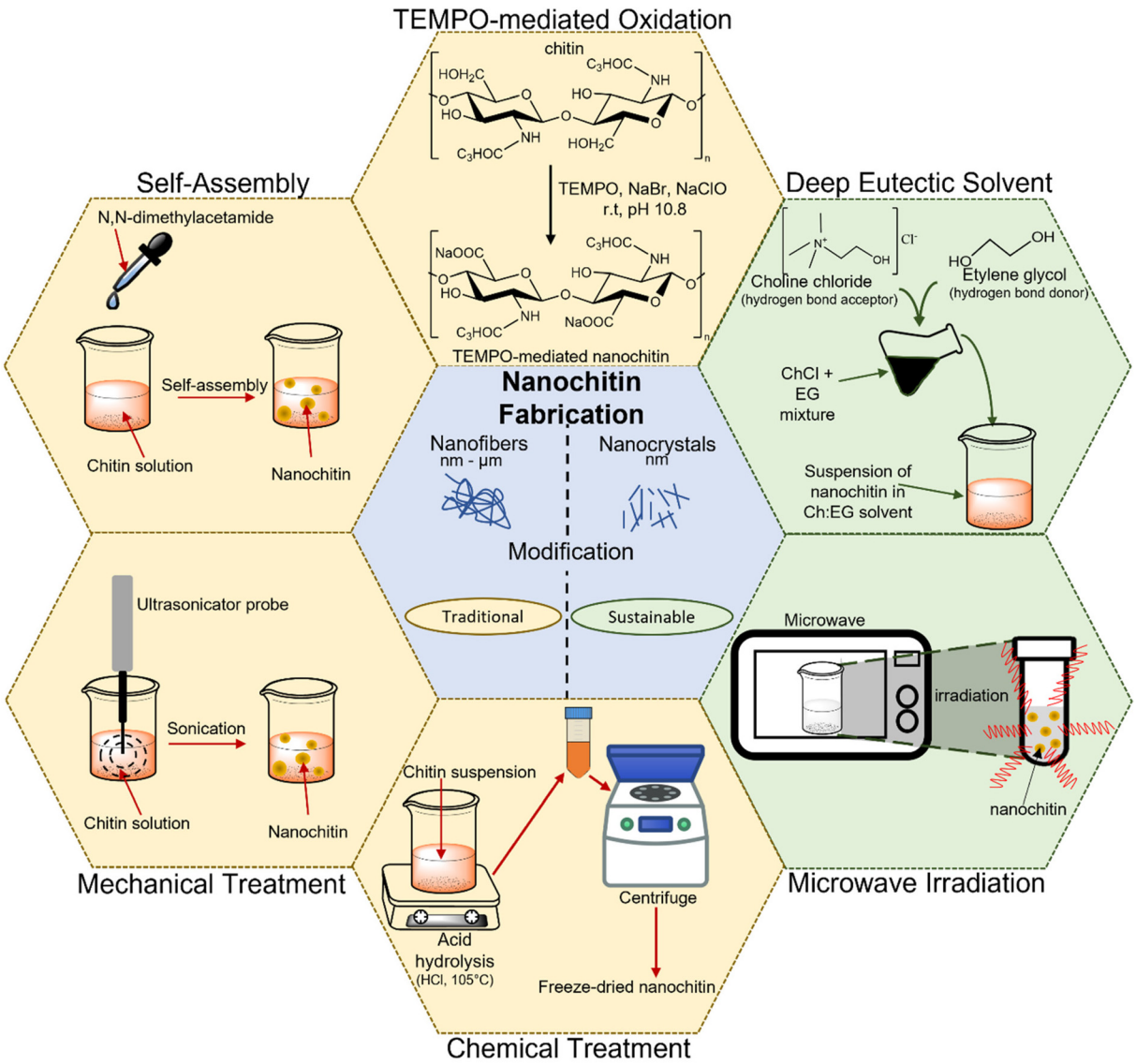

Fig. 4 Various types of methods for the synthesis of nanochitin.

nanochitin are considered the traditional approaches. These are either the earliest methods developed for the extraction of nanochitin or the methods that emphasize efficiency and yield. These techniques can be further classified into top-down (*i.e.*, chemical treatment, mechanical treatment, and TEMPO-mediated oxidation) and bottom-up approaches (*i.e.*, electrospinning, wet spinning, and self-assembly method). In the former, the synthesis of nanoparticles is performed by break-

ing down the bulk material, whereas in the latter, they are created from small building blocks.

3.1.1 Chemical treatment. Acid hydrolysis has been widely explored as an effective method to obtain nanochitin. In the acid hydrolysis process, the acid attacks the amorphous region of the chitin, in which the macromolecular chains are packed in a disordered, low lateral ordered arrangement.[25,26] Consequently, the chitin chains are cleaved transversely along the amorphous regions, leaving the high crystalline domains intact and forming nanochitin with a rod-like appearance.[27] Chitin nanowhiskers were created by Marchessault in 1959 by the acid hydrolysis of chitin using 3 M hydrochloric acid (HCl), while illustrating the liquid behaviour of these nanocrystals.[28] To effectively hydrolyze chitin, Revol and colleagues increased the temperature of the acidified suspension to its boiling point and agitated it.[29] The reaction was quenched by adding distilled water, and the suspension was centrifuged or filtered to remove the acid solution. Subsequently, the suspension was dialyzed to neutral pH using distilled water to completely remove the presence of residual acid and stored it for further use. Although the acid hydrolysis technique involves the use of strong acid solution such as hydrochloric acid (HCl) or sulphuric acid (H_2SO_4), it was realized that the crystalline region of chitin completely dissolves as the acid concentration increases beyond 8.5 N.[28] Since this discovery, numerous studies have attempted this acid hydrolysis method (ranging from 2.5 to 3 M HCl and 1.5 to 6 h hydrolytic time) on various sources of chitin (squid pen,[30] *Riftia* tubes,[31] crab shells[32,33] and shrimp shells[34,35]) to produce nanochitin with a length varying from 50 to 600 nm and width in the range of 8 to 50 nm.

For instance, Li and colleagues effectively isolated the crystalline region of nanochitin from shrimp chitin powder *via* HCl hydrolysis and obtained rod-like nanoparticles with a length of 50–150 nm and width of 30–50 nm.[36] Similarly, Zhou *et al.* also extracted nanochitin from shrimp chitin powder and obtained a slender rod with sharp points with a broad distribution of 100–150 nm in length and 15–30 nm in width.[37] Qin and team replaced HCl with H_2SO_4 to produce nanochitin and attained size in the range of 100 to 400 nm in length and 10 to 50 nm in width.[38] This procedure enables sulphate half-ester functionalities to be present at the nanochitin surface. It is undeniable that acid hydrolysis is effective in generating nanochitin. However, the handling of corrosive chemicals and the generation of wasteful effluents are undesirable and detrimental with respect to sustainable development.

3.1.2 Mechanical treatment. Another strategy that has been extensively utilized for the synthesis of nanochitin is the application of mechanical force. The mechanical treatment involves the application of a high shear force, initiating transverse cleavage along the longitudinal axis of the chitin microfibrillar structure, which is held together by hydrogen bonds, isolating the nanochitin fibers.[39–41] Grinding and ultrasonication are some of the few examples of mechanical treatment techniques that can be used separately or in combination with other treatment techniques such as acid hydrolysis to produce nanochitin.

The grinding process involves breaking down the hierarchical structure by using shearing forces produced by two countersense rotating grinding stones.[42] For the chitin to be effectively fibrillated during the grinding process, an acidic environment is required. This is because a small percentage of amino groups in chitin becomes cationized when acid is added, which aids the fibrillation of chitin through electrostatic repulsion.[43] A study was conducted to compare the chitin nanofibers obtained from a 1% slurry of crab shell chitin that was passed through a grinder with and without acetic acid.[44] It was found that due to the strong hydrogen bonding between the chitin networks, it is challenging to fibrillate chitin without the presence of acid, leading to the formation of large, dense bundles of chitin nanofibers. Although an acidic environment is necessary for the grinding process to create chitin nanofibers, this condition may not be ideal for the production of certain nanocomposites, electrical devices, and biological materials. Hence, Ifuku and team attempted to produce chitin nanofibers *via* grinding under neutral condition, and they succeeded in extracting chitin nanofibers from prawn shell chitin with a consistent diameter of around 10–20 nm.[43]

Ultrasonication is another popular technique used for producing nanostructured materials, where the high energy generated induces the formation, growth, and rapid collapse of cavities in water.[45] Typically, cavitation produces energy in the range of 10 to 100 kJ mol^{-1}, which is equivalent to the energy level of hydrogen bonds.[46] Therefore, the formation of chitin nanoparticles *via* the ultrasonication process is due to the rupturing of the strong hydrogen bonds between the network of chitin. Lu and colleagues extracted chitin nanofibers from dried prawn shell chitin *via* the high-intensity ultrasonication method at an optimal parameter of 60 kHz, 300 W and pH 7.[47] The extent of the breakage of the weak van der Waals forces and hydrogen bonding in the fibers was found to vary with the ultrasonication duration, which allowed the diameter of the chitin nanofibers to be controlled in the range of 20 to 200 nm. The results showed that after 30 min of sonication, high-aspect-ratio nanofibers were obtained with a consistent width of 19.4 nm.

3.1.3 TEMPO-mediated oxidation. An extensively studied and but expensive method utilizes the typical piperidine nitroxide free radical 2,2,6,6-tetramethylpiperidine-1-oxide (TEMPO). The –OH groups at the C6 position of chitin can be selectively oxidized to C═O groups in the presence of the TEMPO/co-oxidation system, producing chitin nanofibers. Fan and colleagues developed a method utilizing TEMPO-mediated oxidation to selectively oxidize the amorphous region of chitin through the radical oxidation pathway.[48] Basically, this technique involves several steps, as follows: (i) chitin is suspended in water containing TEMPO and sodium bromide (NaBr) before sodium hypochlorite (NaClO) solution is added to initiate the TEMPO-mediated oxidation of chitin. (ii) Sodium hydroxide (NaOH) is continuously added to maintain the pH at 10 at room temperature. (iii) To stop the oxidation process, ethanol is added to the solution without using any alkali.[49] In

a study, β-chitin isolated from tubeworms was subjected to TEMPO/NaClO/NaBr oxidation at pH 10 to produce chitin nanofibers with a width in the range of 20–50 nm and length of over few microns.[50] It was found that increasing the amount of NaClO caused the length of the chitin nanofibrils to become shorter. Most of the β-chitin was oxidized to carboxyl groups and transformed into water-soluble sodium chitin salt when an adequate amount of NaClO was added. A similar observation was noted in another independent study, in which higher NaClO concentrations resulted in shorter chitin nanofibrils, which was potentially caused by the intensification of the depolymerization reaction at the ends of the chitin nanofibrils.

Chitin can only be oxidized by the TEMPO/NaClO/NaBr system in an alkaline environment. Alternatively, for the first time, Pang and team successfully produced chitin nanofibers with a width of 5–10 nm and length of 200–400 nm by employing the TEMPO/$NaClO_2$/NaClO system in a mildly acidic environment.[51] They suspended chitin in a pH 6.86 sodium phosphate buffer solution containing TEMPO, sodium chlorite ($NaClO_2$) and NaClO to produce chitin nanofibers *via* oxidation reaction. A similar TEMPO technique with acidic conditions was used by Jiang *et al.* to create chitin nanocrystals with dimensions of 200–600 nm in length and 6–15 nm in width.[52]

3.1.4 Deacetylation pretreatment. Fan and team produced chitin nanocrystals using a different approach, which involves mechanically treating partly deacetylated chitin fibrils at low pH.[53] The partly deacetylated chitin fibrils consisted of an increased number of C2-primary amino groups on the crystal fibers surface. This led to a greater cationic charge density from the protonation of the amino groups, which stabilized the dilute colloidal dispersion of the chitin nanowhiskers due to the enhancement of the electrostatic repulsion between the fibrils. In an acidic environment, this repulsion aids the disintegration of the chitin fibrils during the mechanical process and produces chitin nanocrystals. The acid-degraded chitin dispersion may also experience an isotropic–anisotropic nematic transition when dewatered to an increased concentration.[54] This method involves three primary steps, as follows: (i) the partial deacetylation of chitin, where chitin is added and stirred in 33% (w/w) NaOH solution consisting of $NaBH_4$ and heated at 90 °C for 1–4 h to prevent alkaline depolymerization and weight loss. Subsequently, the chitin solution is centrifuged to neutralization after being rinsed several times with distilled water. (ii) It is subjected to mechanical disintegration, where the chitin solution is adjusted to pH 3–4 by using acetic acid solution and vigorously stirred for 5 days. Finally, (iii) sonication step, where the mixture is sonicated for one minute using an ultrasonic homogenizer. Xu *et al.* utilized this method to prepare partially deacetylated α-chitin nanofibers from crab shell flakes to formulate high-strength membranes with nanocellulose and F-SiO_2 suspensions.[55] The approximate width of the nanochitin was in the range of 10 nm to 20 nm, whereas the length was in the range of 400 to 600 nm.

3.1.5 Electrospinning. Electrospinning technology enables the production of uniformly sized, long nanofibers. During electrospinning, a high voltage is applied between a conductive plate and a tiny aperture in which a solution or polymer melts travels to produce a non-woven mat of fibers.[56] The only way to prepare chitin nanofibers using the bottom-up approach is *via* electrospinning, where different chitin concentrations have varying impacts on the formation of electrospun nanofibers.[57] However, chitin is insoluble in most solvents such as water, organic solvents, acidic and alkaline solution and can only dissolve in 1,1,1,3,3,3-hexafluoro-2-propanol (HFIP).[58] According to Street *et al.*, chitin was dissolved in HFIP solution and electrospun under the optimum conditions (voltage of 17 kV, flow rate of 1.0 mL h^{-1}, relative humidity of 21%, temperature of 23 °C and distance between the tip and collector of 10 cm).[59] It was found that the tensile strength of the nanofibers increased by 30% using the electrospinning method compared to randomly collected fibers. However, HFIP is highly toxic, which restricts its use in electrospinning. Therefore, to enhance the solubility of chitin, it is advisable to lower the molecular weight by utilizing methods such as Co60 gamma ray, microwave irradiation, and ultrasonic treatments. To increase the solubility of chitin, Min *et al.* depolymerized chitin using Co60 gamma rays before dissolving it in HFIP solution for electrospinning. The obtained chitin nanofibers possessed a diameter in the range of 40 to 640 nm and average diameter of 110 nm.[60]

3.1.6 Wet spinning. Wet spinning is another example of a dissolution–regeneration method, which involves dissolving chitin, and then using it as a precipitating agent to regenerate chitin molecules into nanofibers. To produce nanochitin fibers with high aspect ratios, it is possible to use the wet spinning method, where the effect of spinning depends on the concentration of chitin. According to the experimental findings, chitin solutions with higher concentrations gelled more quickly compared to lower concentrations, where they coagulated too slowly for spinning.[61] Additionally, the wet spinning approach may be utilized to spin both chitin composite solutions and pure chitin solutions.[62,63] However, wet spinning has restricted applications due to the limited solvents for chitin. Thus, to fully exploit wet spinning for the generation of chitin nanofibers, it is crucial to develop environmentally friendly solvents that can dissolve chitin.

3.1.7 Self-assembly. The self-assembly method may also be used to create nanochitin, which allows solvents to easily dissolve chitin by rupturing its hydrogen bonds before it regenerates into nanofibers.[64] The examples of solvents used are 1-allyl-3-methylimidazolium bromide (AMIMBr), sodium hydroxide/urea, hexafluoro-2-propanol (HFIP) and *N*,*N*-dimethylacetamide (DMAC). In a study, two different solvents (HFIP and LiCl/DMAC) were used to dissolve chitin to produce nanofibers. The chitin dissolved in HFIP solution produced nanofibers with a diameter of 2.8 ± 0.7 nm using the solvent evaporation technique, whereas the chitin dissolved in LiCl/DMAC solution produced nanofibers with a diameter of 10.2 ± 2.9 nm by the precipitation of the fibers with water.[65] According to Duan *et al.*, chitin nanofiber microspheres were created *via* a thermally induced self-assembly process in

NaOH/urea solution.[66] Commonly, urea hydrates surround the NaOH hydrogen-bonded chitin complex to create a water-soluble sheath-like structure, which causes the chitin to dissolve. However, high temperature destroys the urea-NaOH sheath, which leads to the vigorous aggregation of the chitin chains in a parallel manner and results in the formation of nanofibers with an average diameter of 27 nm.

3.2 Sustainable approach

The increasing occurrence of extreme weather, global warming and rising water levels has attracted significant attention, and consequently it is necessary to find sustainable means consider the consequences of unsustainable development. In this case, nanotechnology is employed by researchers to improve and achieve cleaner and more environmentally friendly processes. To date, different approaches for the synthesis of nanochitin have been attempted, ranging from employing more environmentally friendly processes and using greener solvents to accelerating the reaction to save energy, which will be discussed in more detail in this section.

3.2.1 Microwave irradiation. The microwave irradiation technique is a sustainable approach to extract nanochitin. This technique involves the exposure of a polar solvent sample to an electromagnetic field, where the dipoles of the molecules from the sample attempt to align themselves, which results in friction and collisions, leading to an increase in the temperature.[67] Fernández-Marín *et al.* described using the microwave irradiation approach to manufacture nanochitin from chitin obtained from shrimp, lobster, and squid. Both the lobster and shrimp samples produced rod-shape-like nanochitin with shorter lengths and widths compared to the nanochitin from the squid samples, which had long, fibrillar structures.[68] By using microwave-assisted extraction, the reaction time can be reduced. For instance, depending on the chitin source, the time may be reduced to 10–30 min compared to 90–180 min needed for conventional chemical acid hydrolysis, and the HCl concentration can be reduced from 3 M to 1 M.

3.2.2 High-pressure homogenization. High-pressure homogenization is a procedure that exerts intense pressure on the suspension and separates it into smaller-size particles.[69] High-pressure homogenization is a straightforward and environmentally friendly technique, which was used by Salaberria *et al.* to extract chitin nanofibers from yellow lobster chitin.[70] This procedure involves the ejection of a chitin suspension at high pressure *via* a homogenizing valve, which effectively reduces the size of the chitin nanofibers to less than 100 nm in diameter and several micrometers in length.[70] Recently, chitin nanofibers were produced from chitin isolated from raw crustacean exoskeletons using an atomizing technique known as the high-pressure waterjet (HPWJ) system. The aqueous counter collision (ACC) method and Star Burst method are the two techniques that use the HPWJ system. In the ACC technique, the chitin suspension is passed through a set of nozzles at a pressure of 50–270 MPa, producing a set of jets.[71] Hence, adjusting the pressure and the number of ejecting steps will result in repeated collisions of the sample, reducing the size of the chitin particles in the sample. Kose and Kondo produced chitin nanofibers with a width of 10–20 nm from chitin powder using this technique.[72] Ishida *et al.* synthesized chitin nanofibers with an average width and length of 10 ± 6 nm and 2300 ± 1000 nm, respectively, using the nano-pulverization process with an ACC system of 200 MPa pressure and 60 passes of ejecting steps.[73] The Star Burst technique involves compressing a chitin slurry by a hydraulic piston, which is then passed through a nozzle at high pressure (245 MPa) and the chitin is atomized by colliding with a ceramic ball in the chamber.[74] By using the Star Burst method, Ifuku and team successfully synthesized chitin nanofibers from dry chitin powder.[75] The chitin slurry was ejected through a 100 μm diameter nozzle, under high pressure of 245 MPa, which was repeated for 1, 5 and 10 cycles. With the increased number of passes, the chitin slurry became more transparent and more fibrillated. In fact, the chitin slurry was already noticeably fragmented after the first cycle under acidic condition. In contrast, the chitin slurry had to undergo more passes under neutral condition to achieve average widths of 18.2 m and 17.3nm for 5 and 10 passes respectively.

3.2.3 Ionic liquids. Ionic liquids (IL) are viewed as environmentally friendly salts, which melt below 100 °C and are made completely of anions and cations.[76] These substances have been suggested as an alternative to organic and aqueous solvents for the dissolution and swelling of biomass. These IL solutions containing chitin can be used to create chitin nanofibers *via* the electrospinning method. In a study, the chitin isolated from raw crustacean shells was dissolved by the ionic liquid 1-ethyl-3-methylimidazolium acetate, which was immediately spun into fibers and films. Many researchers used similar methods to produce chitin nanocrystals, where chitin was first gelated with AMIMBr, and then regenerated with methanol. More specifically, the resultant gel was briefly immersed in methanol, and then sonicated to create a suspension of chitin nanocrystals. In a study, chitin nanocrystals with dimensions of 20–60 nm in width and several 100 nm in length were produced and utilized as a suspension to create a film by the filtration method.[77]

3.2.4 Deep eutectic solvents. Deep eutectic solvents (DESs) are known as a type of green solvent that consists of high, non-symmetric ions with low lattice energy, and hence low melting point. A quaternary ammonium salt or hydrogen bond acceptor (HBA) and a metal salt or hydrogen bond donor (HBD) are often complexed to produce DESs.[78] This complexation causes charge delocalization through hydrogen bonding, which aids to decrease the melting point of the mixture.[78] DESs have always been misunderstood and referred to as IL analogs due to their similarities to ILs such as high solvent capacity and low vapor pressure. However, DESs are less expensive, more accessible, non-toxic, recyclable, biodegradable and easier to produce than ILs.

Sharma and team were the first to report that by using conventional heating, microwave heating, and ultrasound-assisted heating, α-chitin could be dissolved in DESs in a 1 : 2 mole ratio for a mixture of choline chloride : thiourea, choline

chloride : urea, chlorocholine chloride : urea, choline bromide : urea and a mole ratio of 1 : 4 for betaine hydrochloride : urea.[79] One year later, Mukesh and colleagues used the same DESs mole ratio mixture as Sharma *et al.*[79] for choline chloride : thiourea and produced chitin nanofibers with a width of 25–45 nm and a length of 162–450 nm.[80] Similarly, chitin nanocrystals were created with a diameter in the range of 42 to 49 nm and a length of 257 to 670 nm by utilizing choline chloride and various acids such as lactic acid, oxalic acid, citric acid, malonic acid, and DL-malic acid in a ultrasound-assisted procedure (Fig. 5).[81] In a different investigation, a green, non-volatile solvent of DES containing choline chloride : zinc chloride with a mole ratio of 1 : 2 was employed to produce acetylated and esterified chitin nanocrystals in a one-step synthesis.[82] Chitin nanocrystals with high yield (≈88.5%) were produced from a betaine chloride : ferric chloride hexahydrate mixture with a molar ratio of 1 : 1.[83]

3.2.5 Enzymatic hydrolysis. Compared to the chemical synthesis approach, biological approaches using a range of microorganisms are viewed to be more environmentally friendly. However, although biological approaches are likely to be the greenest isolation method, their efficiency and cost still need to be improved. Using this technique, nanochitin can be easily obtained by simply incubating chitin with the enzymes, followed by stopping the reaction with either heat or ice and isolating the purified nanochitin. The recent study by Barandiaran *et al.* involved incubating α-chitin flakes with lytic polysaccharide monooxygenase (LPMO).[84] The mixture was put on ice to halt the reaction upon completion. The isolation of nanochitin was performed by using ultrasonication, centrifugation and lyophilization. After 72 h of incubation, the nanochitin obtained had a length and diameter of 458 nm and 32.3 nm, respectively. The cleavage site was determined to be the β-(1 → 4) glycosidic bond, where C1 and C4 were selectively oxidized. In another study, chitinase was used together with ultrasonication to prepare nanochitin fibers.[85] Upon completion of the reaction, heat was applied to the mixture to stop the reaction. The purified nanochitin was obtained after ultrasonication and lyophilization were applied to the mixture. The results were promising with the length of the attained nanofibers varying from 130 nm to 195 nm depending on the duration of the enzymatic hydrolysis. Other factors that can affect the efficacy of the enzymatic hydrolysis include the environmental environment and the enzyme concentration (Table 2).

3.3 Sustainable analysis of nanochitin extraction

Globally, energy and environmental concerns have reignited scientific interest in the development of materials derived from biomass, which are more sustainable than materials derived from fossil fuels. However, besides demonstrating desirable functionalities, it is necessary to perform a life cycle assessment (LCA) for nanochitin to quantify the sustainability of this nanobiopolymer.[93] LCA is an established methodology to evaluate the environmental impact of the technology of interest from cradle to grave. The process to perform LCA involves three general steps (Fig. 6). Firstly, the scope of the study needs to be defined, which includes the boundaries and limitations. Secondly, the quantitative inputs (energy, resources, chemicals, *etc.*) and outputs (emissions/waste to the environment) during the life cycle of the processes involved will be modelled. Lastly, the impact analysis is conducted by converting the model data to interpretable environmental impacts, which are categorized into midpoint and endpoint indicators. Midpoint indicators focus on the short-term impacts, such as climate change, terrestrial acidification, and water depletion. Alternatively, endpoint indicators focus on the long-term eventual impacts, such as damage to human health, the ecosystem and resource availability.

Generally, there are various factors that can affect the environmental impact score of the technology.[93] Firstly, the raw material determines the chitin content, and thus the extent of chemical treatment required. Simultaneously, the raw material determines the resource availability and accessibility. Secondly, the isolation techniques of nanochitin can have different levels of impact, for example, replacing the use of concentrated hydrochloric acid (HCl) and sodium hydroxide (NaOH) will reduce the environmental impact. Thirdly, the manufacturing of nanochitin-based products has various extents of impact, which differ greatly according to the applications (biomedical, agricultural, catalysis, *etc.*). LCA is necessary to quantify the relative impacts of each factor. Presently, most of the reported nanochitin production processes are still at low technology readiness levels (TRL), and hence no comprehensive LCA has been conducted on this nanomaterial. Nonetheless, there are some reported LCAs that are relevant to provide a useful reference point for future studies.

Muñoz and co-workers presented a cradle-to-gate LCA of the production of bulk chitosan, which was derived from chitin *via*

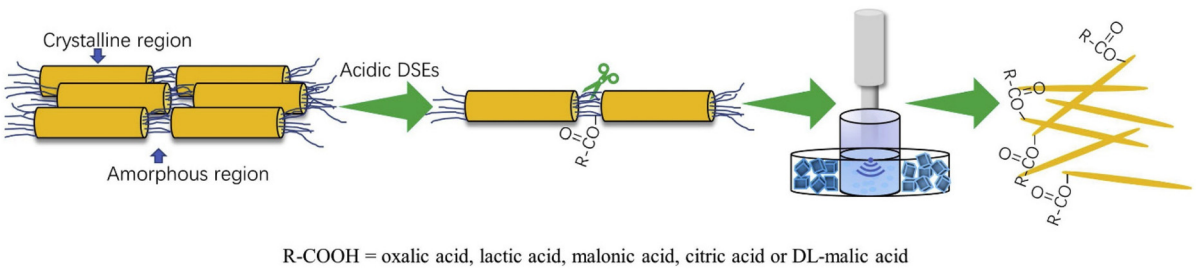

Fig. 5 Illustration of nanochitin synthesis using organic acid DESs. Reproduced with permission.[81] Copyright 2020, Elsevier Ltd.

Table 2 Summary of the sources and methods for the preparation of nanochitin

Type of nano chitin	Typical source	Formation process	Characteristics			Application	Ref.
			Length/nm	Width/nm	Diameter/nm		
Nanocrystals	Shrimp	Acid hydrolysis, ultrasound	300	60	—	Films for food coating and packaging	86
Nanofibrils	Crab	Acid hydrolysis, homogenization, ultrasound	150–200	5–10	—	Antimicrobial film for packaging	87
Nanocrystals	Cuttlefish bone	Acid hydrolysis, ultrasound	22	14	—	—	88
Nano whiskers	*Rifia* tubes	Acid hydrolysis, ultrasound	500–10^4	18	—	Nanocomposite films	31
Nanofibrils	Tubeworm, pens of squid	TEMPO-mediated oxidation	Several microns	20–50	—	Translucent gel	50
Nano whiskers	Crab shells	TEMPO-mediated oxidation, ultrasound	150–500	20–55		For fuel cell applications	89
Nanofibers	Chitin powder	Electrospinning method	—	—	163	For wound healing and regeneration of oral mucosa and skin.	90
Nanofibers	Chitin powder	Electrospinning, ^{60}Co gamma ray, deacetylation	—	—	40–640	Nanofibrous matrices	60
Nanofibers	Crab shell	Ultrasound	650	9–120	—	Textile industry for antibacterial finishing application	91
Nanofibers	Crab shell	Grinding	—	10–20	—	Nanomaterials	44
Nanofibers	Chitin powder	Grinding, HPWJ treatment	—	—	—	Nanofibrous matrices	40
Nanocrystals	Crab shell	TEMPO-mediated oxidation, partial deacetylation, starburst	250	15	—	Zwitterionic nanocrystals for biomedical field	49
Nanocrystals	Shrimp shells, squid pens, yellow lobster	Acid hydrolysis, microwave irradiation	314–900	41–42	—	—	68
Nanowhiskers	Crab shell	Partial deacetylation	250	6.2	—	Nano-composite materials for reinforcement	53
Nanofibers	Chitin powder	Self-assembly	—	—	2.8–10.2	Nanofibrous matrices	64
Nanocrystals	Shrimp shells	Deep eutectic solvent	100–700	20–80	—	—	82
Nanofibers	Shrimp shells, practical grade chitin powder, pure chitin powder	Ionic liquid	—	—	—	Film for medical application	92
Nanofibers	Chitin powder	Dissolution–regeneration			3×10^4–9×10^4	Nonwoven mat for wound dressing	61
Nanofibers	Crab shell	TEMPO-mediated oxidation, aqueous counter collision	492–828	—	—	Hydrogel with enhanced mechanical properties for various application	71
Nanofibers	Shrimp fragment powder	Partial deacetylation, high-pressure homogenization	400–600	10–20	—	Waterproof packaging, waterproof transparent membrane	55
Nanocrystals	Chitin powder	Enzymatic hydrolysis	458	—	32.3	For biomedicine such as tissue engineering and bioprinting	84
Nanofibers	Crayfish shell	Enzymatic hydrolysis, ultrasound	130–195	—	—	For emulsions	85

an additional deacetylation process.[94] This study assessed the primary data from two producers located in India and Europe that produce chitosan for general purposes and medical use, respectively. Given that these two chitosan productions involve different supply chains, production locations and different uses, it was expected that they would have distinct environmental profiles. In the case of the Indian-produced chitosan (Fig. 7a and b), the major impact of chitin production (from shrimp shells) on climate change and acidification was related to the use of HCl and the ammonia emission from the use of protein-rich sludge as fertilizer. The HCl and NaOH treatments also have a significant impact on ecotoxicity and water quality. Regarding the European-produced chitosan (Fig. 7c and d), chitin (from crab shells) was sourced and produced from China. Given that coal is the main fuel used for heating and electricity in China, energy generation was identified as the main contributor to the impact on climate change, acidification and ecotoxicity. Notably, the acquisition of crab shells for chitin production resulted in a credit in the acidification impact indicator as the crab shells were diverted from being composted, thus avoiding ammonia and NO_x emissions. This avoidance in acidifying emissions was actually more significant than the emissions associated with the production of chitin, *i.e.*, a net reduction of acidification can be achieved through the production of chitin. This work highlights

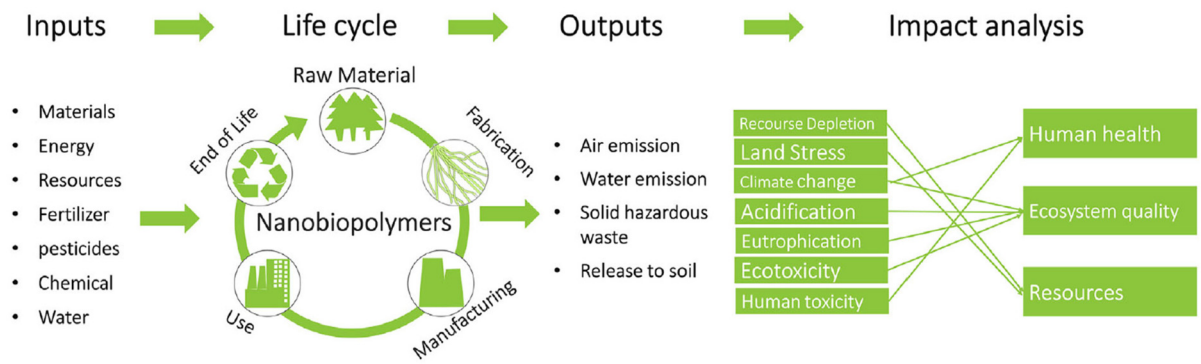

Fig. 6 General process of LCA for nanobiopolymers such as nanochitin. Reproduced with permission.[93] Copyright 2018, John Wiley and Sons.

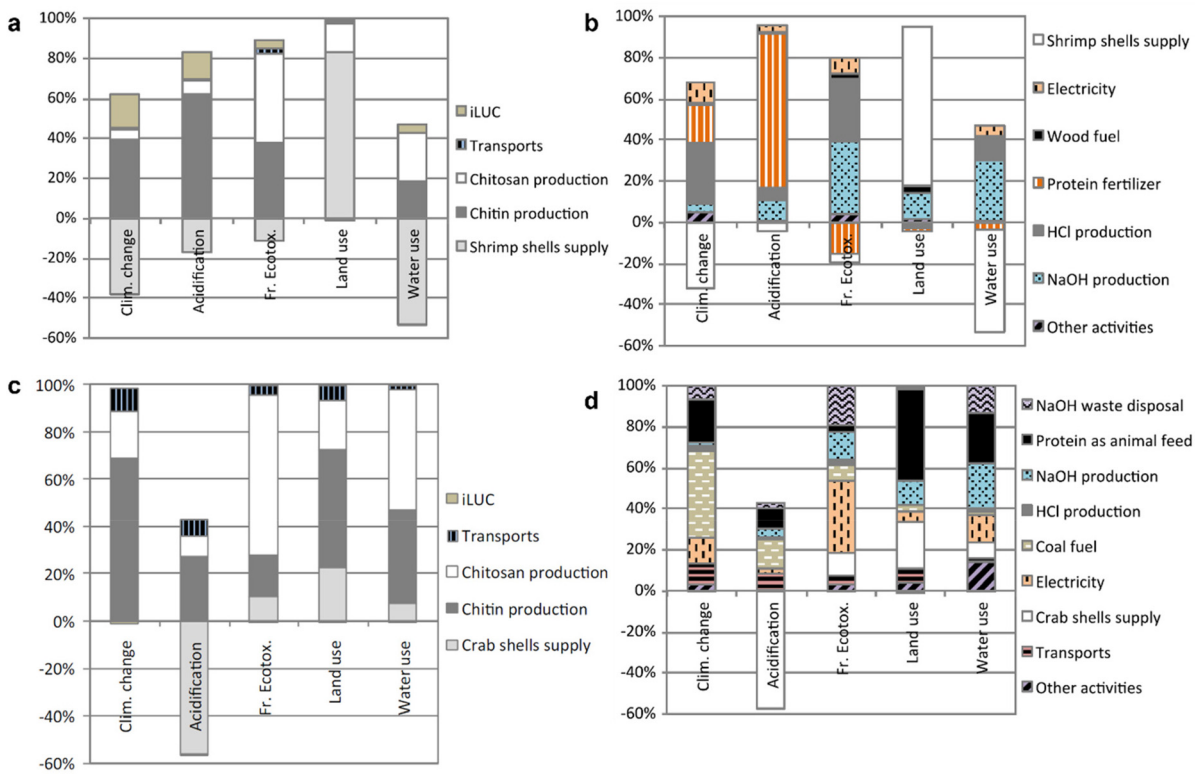

Fig. 7 Impact assessment disaggregated into individual activities for the production of chitosan in (a and b) India and (c and d) Europe. Reproduced with permission.[94] Copyright 2018, Springer Link.

the important factors that can contribute to the global environmental impacts for chitosan (and thus, chitin) production, hence providing a useful benchmark for future investigations, although there will be some differences in chitin production on the nanoscale.

Cinelli *et al.* conducted an LCA study on a bio-plastic-based on polylactic acid and chitin nanofibrils (CNF).[95] In the analysis of CNF production, the energy associated with the concentrating process of the CNF suspension, *i.e.*, drying of water, was the main factor affecting the overall evaluation. Thus, the authors suggested the direct production of a concentrated CNF suspension of 20 wt% (*vs.* the original 2 wt%) to avoid the energy-intensive purification step. However, additives will be further required to aid the dispersion of CNF in the concentrated suspension, which may cause a change in bio-plastic properties or require additional steps to remove the additive present at a later process stage. Alternatively, the use of less energy-intensive separation methods, such as membrane filtration, can also be explored to concentrate the CNF suspension. It is important to note that this LCA is specifically for the production of CNF-containing bio-plastics, and therefore the requirement for the preparation of concentrated CNF suspension may not be applicable for other nanochitin materials with different applications.

As the production of nanochitin advances to a higher TRL, it will be increasingly crucial to evaluate the ecological footprint of these emerging materials through comprehensive LCAs. Additionally, LCA will be an important tool to provide a quantifiable justification for the sustainable production of chitin from alternative sources (crustaceans *vs.* insects *vs.* fungi).

4 Nanochitin applications towards advanced manufacturing

Advanced manufacturing can be defined as the adoption of innovative or cutting-edge technology in production, either to improve the process or product. The reduction of chitin to the nanoscale has seen the emergence of ingenious technology. In the nanoscale form, nanochitin gains new properties such as higher reactivity that arises with higher aspect ratio and new interaction with light. Besides the recently gained advantages, nanochitin still maintains the attributes as its predecessor, which makes it attractive for use in various sectors ranging from 3D printing and photonics to packaging and catalysis. This section summarizes the recent works on nanochitin in each field.

4.1 Nanochitin for 3D printing

Recently, nanochitin has gained popularity in three-dimensional (3D) bioprinting applications. 3D bioprinting is a method of additive manufacturing that utilizes biocompatible filaments that may or may not be cell-laden to produce complex, tissue-like constructs by layer-by-layer deposition.[96,97] Nanochitin provides biocompatibility and biodegradability to 3D bio-printed constructs used in regenerative medicine and tissue engineering. The high aspect ratio of nanochitin allows it to enhance the mechanical strength of objects constructed using bioinks, making it an attractive candidate as a filler in bioinks.[98,99]

Karimipour-Fard *et al.* synthesized a nanocomposite filament of polycaprolactone (PCL) matrix with nano-hydroxyapatite (n-Hap) and ChNW fillers using a 1-butyl-3-methylimdazolium chloride (BMIMCl) ionic solvent. A preosteoblast mouse bone cell line was used to investigate the applicability of the nanocomposite filament for tissue engineering. It was found that ChNW increased the mechanical properties and the biodegradation rate of the PCL/n-Hap/ChNW filaments and enhanced the cell attachment and proliferation.[100]

Sadhasivam *et al.* fabricated a nanocomposite filament of poly(butylene adipate-*co*-terephthalate) (PBAT) and nanochitin filler for injection moulding. Similarly, nanochitin improved the thermal and mechanical properties of the PBAT/nanochitin filament, with the optimum composition being 30% nanochitin. 3D constructs made from the PBAT/nanochitin filament were stable and expected to be biodegradable. The PBAT/nanochitin nanocomposite was shown to promote cell migration in a scratch wound assay and exhibited *in vivo* non-toxicity in a zebrafish embryo model.[101]

Ling *et al*. utilized gelatin methacrylate (GelMA) and chitin nanocrystal to develop a biomaterial ink for 3D bioprinting.[102] The addition of 1% (w/v) chitin nanocrystal is sufficient to significantly enhanced the properties of 10% (w/v) GelMA. For example, in terms of mechanical properties, printability, cell adhesion and proliferation. Yet, the chitin nanocrystal introduction did not alter the porosity which is important for tissue engineering as the pores are necessary to facilitate nutrient transport, cell attachment, migration and proliferation.

In another study, Zhang *et al.* designed an *in situ* self-assembling bioink made of fumed silica (FS) and nanochitin for 3D printing. Nanochitin enabled the FS/nanochitin bioink to display the mechanical, viscoelastic, and rheological properties required for 3D printing. 3D objects printed with the optimal concentration of 5–8 wt% nanochitin in the bioink possessed high structural fidelity and the ability to support their own weight after extrusion. The 3D scaffolds printed using this FS/nanochitin bioink were elastic and could return to their original shape after being subject to multiple deformations.[103]

4.2 Nanochitin for photonic applications

Native photonic chitin structures can be found in natural occurring species such as crustaceans and insects.[104] Due to the periodic ordered chitin exoskeleton, the chitin micro/nano-structure interacts with light selectively and displays bright iridescent colors.[105,106] To mimic these photonic structures, scientists explored the use of the exoskeleton of these creatures as a template for replication (Fig. 8).

Several studies have utilized butterfly wings as a bio-template for the *in situ* growth of metal nanoparticles. Boruah *et al.* deposited sliver ions (Ag^+) in the chitin layers of a *Pieris brassicae* butterfly wing, and subsequently converted them into sliver (Ag) nanoparticles.[107] The wings were soaked for varying durations and their photonic band gap was studied. The band gap opening was determined by the interactions between the localized surface plasmon of the Ag nanoparticles and homogenous air-hole structure on the butterfly wing. The photonic band gap could be tailored by adjusting the Ag adsorption time. An increase in the soaking time resulted in the reflectance peak maximum shifting from 335–355 nm to 680–730 nm. Mu *et al.* utilized the chitin/chitosan found on butterfly wings for reduction to synthesize gold (Au) nanoparticles *in situ* and presented their application as surface enhanced Raman spectroscopy (SERS) substrates.[108] The butterfly wing from *Morpho menelaus* was employed to detect 4-ATP at the lowest concentration of 10^{-9} M and exhibited the lowest RSD among the samples. Using the forewing of *Troides helena* as a biomimetic template, Tian *et al.* modified the chitin from the forewing with amine moieties, and subsequently deposited Au and CuS nanoparticles in the structure.[109] Subsequently, they demonstrated the ability of the obtained chitin to improve the infrared absorption, reduce the reflectance, and infrared (30.56%) and solar photothermal conversion ability. Additionally, it achieved a solar absorbance of up to 98% when fabricated into a solar absorber. These fea-

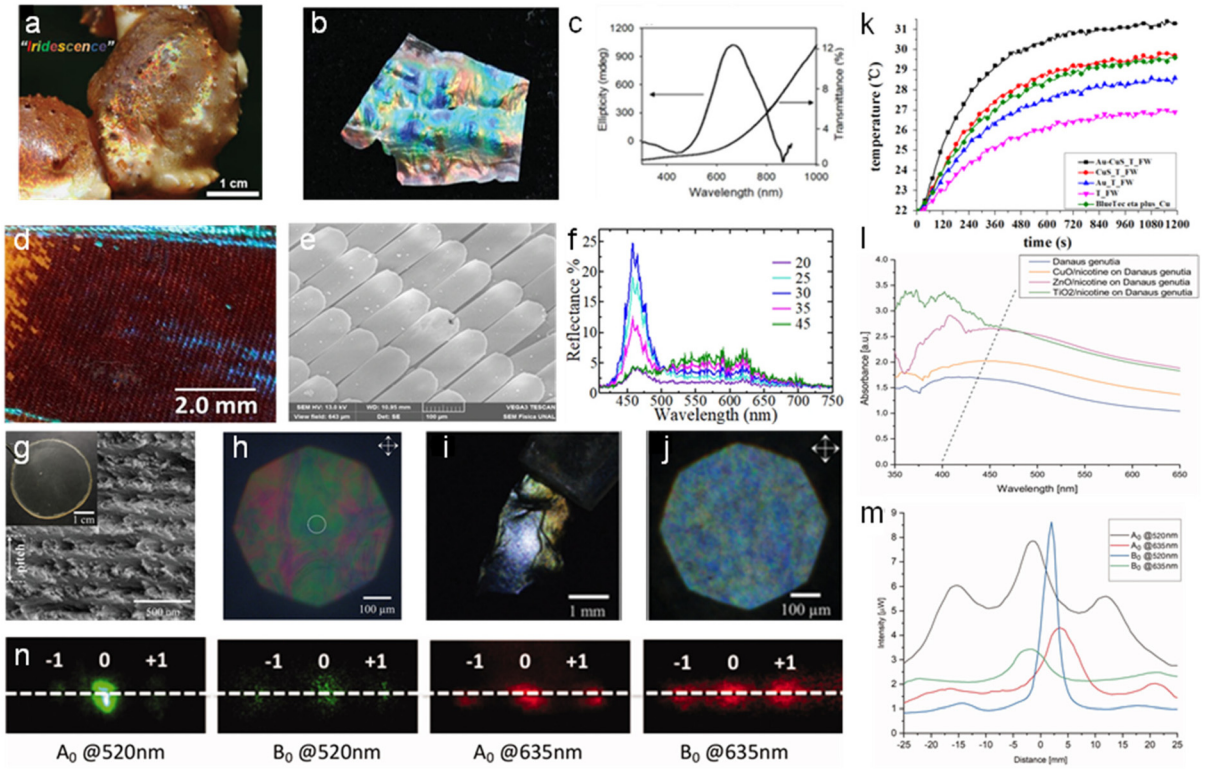

Fig. 8 Nanochitin for photonic applications. (a) Optical image of a snow crab claw displaying iridescence. (b) Photograph of iridescent chitosan membrane derived from snow crab leg shells. (c) UV-vis and CD spectra of chitosan membrane. Reproduced with permission.[112] Copyright 2019, John Wiley and Sons. Optical images of the *M. cypris* Colombian butterfly wing: (d) 1× magnification at 0° about the normal axis, viewed under the microscope. (e) SEM image at the scale of 100 µm. (f) Reflectance spectra of the *M. cypris* butterfly wing as a function of wavelength for the incidence angles of 20°, 25°, 30°, 35° and 45°. Reproduced with permission.[113] Copyright 2020, Springer Nature Limited. (g) SEM image of the cross-section of fungal chitin nanocrystal film (f-ChNC) and the film optical image is shown in the inset. (h) Faint structural coloration observed for the f-ChNC film under the cross polarized microscopy. (i) Image showing strong blue/green coloration of f-ChNC film flake after alkaline treatment. (j) Microscopy image of f-ChNC film flake, highlighting the blueshift of the reflected color. Reproduced with permission.[114] Copyright 2022, John Wiley and Sons. (k) *T. helena* forewings functioned as a biomimetic template to produce a photothermal conversion material under irradiation from a 980 nm laser. Reproduced with permission.[109] Copyright 2015, Elsevier Ltd. (l) Changes in the absorbance of the butterfly wing scales due to the deposition of different metal oxide nanoparticles and nicotine mix. (m) Distribution of the electric field intensity of the butterfly wing scales illuminated by red and green light. (n) Far-field diffraction of butterfly wing scales upon exposure to red and green light. Adapted with permission.[115] Copyright 2022, Informa UK Limited.

tures are associated with the plasmon-to-exciton/plasmon coupling effect between the nanoparticles together with the favorable coupling between adjacent resonant systems in the sub-micrometer antireflection quasi-photonic structures of the forewing.

Chitin powder has also been explored as a starting material for photonic applications. A bio-ink derived from squid pen chitin functionalized with genetically produced amyloid proteins was developed by Wei *et al.*[110] The bio-ink was proven to be applicable for multiple fabrication techniques such as air-brushing, electrospinning, and lithography. Particularly, soft lithography was used to produce ordered and freestanding structures at the micro-level. The potential photonic applications for the fabricated structures as light-guiding gratings include anti-reflection and photonic electrodes. To better understand the natural photonic observations, Liu *et al.* investigated the self-assembly of chitin nanocrystals in capillaries and found that the chitin nanocrystals form a continuous orderly anisotropic phase depending on the phase boundary growth.[111] The air–liquid interface confined at the end of capillaries allowed the concurrent evaporation and deposition of chitin nanocrystals, which self-assemble into nested paraboloid Bouligand structures with a density gradient. Continuous birefringent layers were observed as a result of directional evaporation. This study provided insight into the biological self-assembly process of chitin nanocrystals found in living organisms.

The challenge with the fabrication of natural photonic structure arises from the difficulty in replicating the hierarchal structure without the use of a bio-template. Hence, many studies employed the forewings of butterflies or other species that have photonic architectures as a native photonic template.[116–119] In addition, the stages of chitin biosynthesis that occur in living species require deeper understanding given that it ultimately influences the final morphologies.

4.3 Nanochitin for intelligent food packaging

Nanochitin in the form of nanofibers or nanocrystals has been well exploited as a reinforcing agent in traditional food packaging because of its non-toxicity and hydrophilic nature for the ease of dispersion in various aqueous polymer matrices.[120] It is also known to enhance the physical properties (*e.g.*, mechanical, thermal, and barrier) of films. To advance traditional food packing for the better monitoring and preservation of food, intelligent food packaging capable of providing cues on food freshness is desirable. Anthocyanins are bioactive compounds that give rise to the different colors observed in flowers, fruits, and vegetables.[121] Many studies exploited natural anthocyanins extracted from various plants as the source of pH sensitive pigments. In general, anthocyanins are incorporated into a polymer matrix compatible for food packaging, endowing them with an intelligent feature to change color under different pH environments.[122]

Zheng *et al.* developed two colorimetric films for the evaluation of milk and pork freshness separately (Fig. 9a).[123] The films consisted of a chitin whisker filler, anthocyanins extracted from black wolfberry, and sodium alginate or gelatin matrix. The films could exhibit visible color shifts between pH 3–12. The chitin whiskers could form hydrogen bonding and electrostatic interactions with the functional groups available in the other components, resulting in reduced water solubility, improved thermal stability, and enhanced anthocyanin binding. Depending on the coloration response to extreme acid (*e.g.*, lactic acid) or alkaline (*e.g.*, ammonia) conditions, the films were concluded to be suitable for detecting milk or pork spoilage. In another study, anthocyanin from red cabbage (RCAs) was added to a chitosan (CS)/oxidized-chitin nanocrystal (OCN) matrix by Chen *et al.* (Fig. 9b and c).[124] The RCAs were successfully integrated with CS/OCN *via* hydrogen bonding and color-changing films were formed. The films exhibited a visible color change according to the surrounding pH. When tested in the presence of hairtail (*Trichiurus lepturus*) and shrimp (*Penaeus vannamei*), a color changed from reddish purple (fresh stage) to brown, and lastly yellow (spoiled stage) was observed across 48 h. The color change was strongly correlated with the seafood spoilage process (R^2 > 0.90). Similarly, Sani *et al.* successfully entrapped red barberry anthocyanins (RBAs) in a composite chitin nanofiber (CNF) and methylcellulose (MC) matrix, thus forming a pH-sensitive colorimetric film.[125] pH-Sensitive composite films were used to monitor the freshness of the fish fillets over a period of 72 h. The decomposition process released volatile ammonia and amines, which led to an increase in pH (6.3 to 8), and this was reflected by a colour change in the pH-sensitive film from reddish to pale pink.

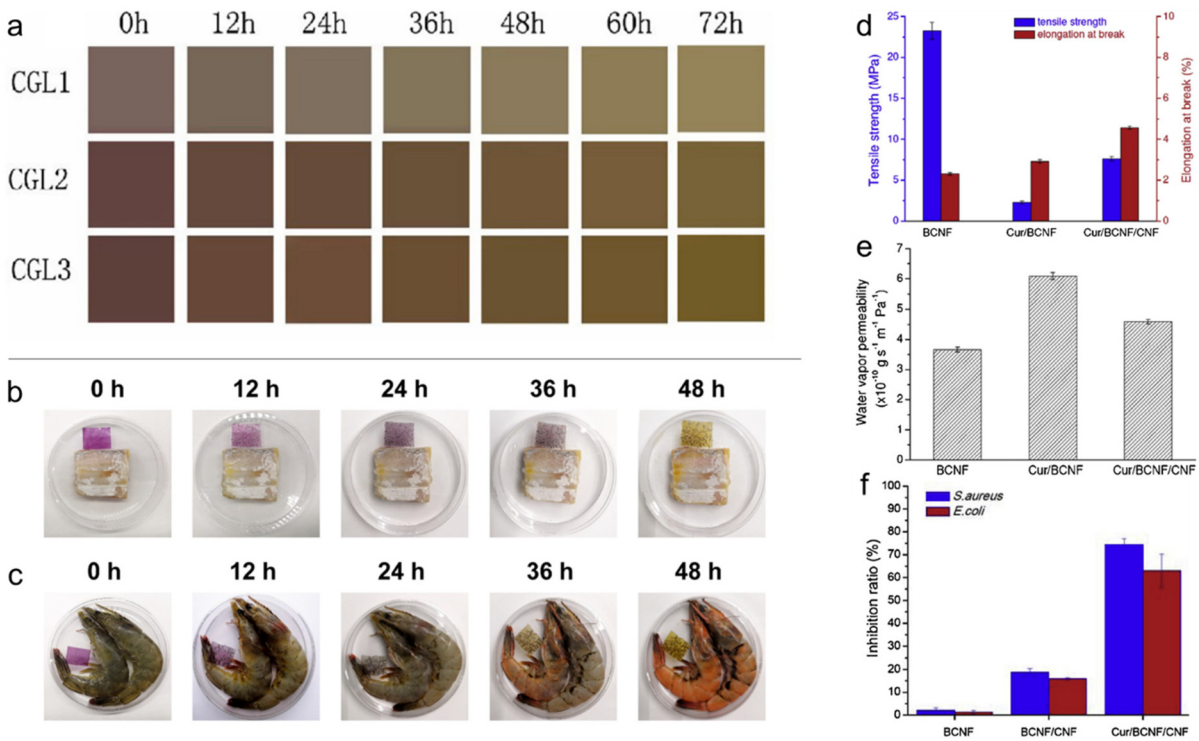

Fig. 9 Nanochitin for food packaging. (a) Real-time images of the color change displayed by the colorimetric films developed with chitin whiskers, gelatin and anthocyanins, when stored with pork samples at 25 °C for 72 h. Reproduced with permission.[123] Copyright 2022, Elsevier Ltd. Color indication captured by COR-1.2 films in response to the freshness of (b) hairtail and (c) shrimp during storage at 25 °C. Reproduced with permission.[124] Copyright 2021, Elsevier B.V. (d) Mechanical strength, (e) water vapor permeability and (f) inhibitory effects of the film samples against bacteria determined using the CFU method. Reproduced with permission.[126] Copyright 2019, Elsevier Ltd.

Besides anthocyanins, compounds such as curcumin, which are pH sensitive, can also provide an observable colour indication for the monitoring of food spoilage. Curcumin (Cur) micro/nanoparticles were formed *in situ* in a bacterial cellulose nanofiber (BCNF)/chitin nanofiber (CNF) composite film, as reported by Yang *et al.* (Fig. 9d–f).[126] With the incorporation of CNF, the Cur/BCNF/CNF film displayed improved mechanical and water barrier properties compared to the Cur/BCNF film. This is due to CNF acting as a reinforcement nanofiller and a hindrance to water diffusion. A colour change from yellow to reddish brown was observed when the pH increased from 1 to 13 when the Cur/BCNF/CNF films were immersed in solutions.

Another pH-sensitive compound that was investigated was elderberry extract. Cabrera-Barjas *et al.* obtained nanofibrous β-chitin from squid pen waste and added glycerol together with elderberry extract of varying concentrations to form intelligent films for fish freshness monitoring.[127] Elderberry is considered a natural sensing pigment, which displays different colors in the presence of acid or alkaline surroundings. The films formed by the combination of nanofibrous β-chitin and elderberry extract exhibited improved tensile strength and elongation at break. As the pH changed from 2 to 12, the film changed color from pink to grey. The combination of these properties makes the film suitable for food monitoring. They tested the film by monitoring the freshness of Hake fish and found that the film transited initially from pink to purple, and subsequently, blue by day 6 due to the increasing basic environment caused by bacteria growth.

More recently, the incorporation of active ingredients to aid the preservation of food was explored by some researchers. These additives provide additional properties such as antioxidant and/or anti-bacteria behaviors. Fernández-Marín *et al.* investigated the addition of curcuma oil and anthocyanin extracted from *Curcuma Longa* L. and red cabbage, respectively, in chitosan/chitin nanocrystal composite films.[128] Curcuma oil and anthocyanins were proven to be pH- and ammonia-sensitive components. The additional actives reduced the moisture content and water solubility and increased the ultraviolet light barrier and mechanical strength. Moreover, they endowed the film with antioxidant characteristics together with color sensitivity to pH and ammonia variations. In another study by Duan *et al.*, pullulan/chitin nanofibers were electrospun with curcumin and anthocyanins as active ingredients.[129] They successfully embedded curcumin and anthocyanins in the PCM substrate. The combination of both actives enhanced the antioxidant and antimicrobial performance of the film compared to the films only containing either component. The films with anthocyanins were proven to exhibit distinct color changes with a change in pH. The PCN/CR/ATH nanofiber composite was tested by monitoring the decay of *Plectorhinchus cinctus* and an observable color change was detected. Recently, natural red cabbage extracts (RCA) and nisin were immobilized in a chitin nanofiber reinforced pullulan/chitosan composite matrix by Wu *et al.*[130] RCA and nisin were well integrated and dispersed and formed hydrogen bonding with the other components in the composite. The inclusion of these active compounds also improved the mechanical strength, thermal stability, water vapor and UV light barrier properties. The composite film exhibited antioxidant and antibacterial capabilities due to the presence of RCA and nisin, respectively. Fresh food monitoring was demonstrated with sea bass (*Lateolabrax japonicus*), whereby the nanocomposite films changed from red (pH 2) to blue (pH 12) over the decay duration.

In summary, nanochitin has been utilized as a reinforcing material to improve the natural limitations such as mechanical strength and barrier properties of polymeric films for food preservation. To provide a clear observable indication of food spoilage, plant-based anthocyanins were exploited as pH-sensitive pigments for intelligent food packaging. Therefore, the combination of both chitin-reinforcing agent and color-changing pH-responsive extracts led to the development of smart films for food monitoring. These films can provide visual indication of food spoilage rate, and simultaneously have suitable physical properties for the preservation of food. Furthermore, to expand the capabilities of these nanocomposite films, additional active chemical compounds can also be incorporated to provide bioactivities, which include antioxidant and antibacterial properties that aid with the preservation of food.

4.4 Nanochitin for green catalysis

Nanochitin is created by breaking down chitin into nanoscale particles using various physical and chemical processes.[1,131–133] Thus, nanochitin possesses a high surface area, together with biocompatibility, biodegradability and low toxicity, making it an attractive material for use in catalytic applications.[134–136] Due to its unique surface chemistry, nanochitin is an attractive material and has been intensively investigated for potential use as a catalyst or as a support for catalytic materials.[137,138] Nanochitin acts as the catalyst support for a wide range of catalysts, covering inorganic catalysts such as metal and metal oxides, as well as organic and biocatalyst such as organic molecules and enzymes.

4.4.1 Heterogeneous inorganic catalyst support. Heterogeneous catalysis systems are highly desirable due to their ease of catalyst/product separation, as well as catalyst recovery and recycling. In this case, one advantage of nanochitin as a supporting material is its biodegradability. Unlike conventional support materials such as carbon and silica, nanochitin can be easily degraded by natural processes, reducing the environmental impact of catalyst synthesis and use. Alternatively, the large surface to volume ratio of nanochitin allows for a high loading of metal nanoparticles and promotes efficient catalyst performance. The surface chemistry of nanochitin can also be modified to enhance its interaction with metal nanoparticles and improve the catalyst stability. Table 3 presents a summary of the common inorganic catalysts hosted by nanochitin in both catalytic chemical reactions and photocatalytic reaction systems.

Heterogeneous support for metal nanoparticles. Nanochitin has several advantages as a support material for metal catalysts, as follows:

Table 3 Summary of nanochitin-supported inorganic catalyst systems

Catalyst	Nanostructure	Reaction scheme	Performance and stability	Ref.
Pd-chitin nanocrystals	Chitin nanocrystals	Heck coupling	• Yield 100%	139
Au-chitin nanofibre membrane	Chitin nanofiber	Reduction of 4-nitrophenol	• As an indicator to show the successful recovery of Au NPs from Au^{3+} in the nanochitin matrix	140
	Chitin nanofiber	Peroxidase substrate 3,3,5,5-tetramethylbenzidine (TMB)	• Useful in the accurate and rapid determination of H_2O_2 • Potentially useful in food, pharmaceutical analysis	
	Chitin nanofiber	Glucose oxidation	• Oxidize the glucose while generate H_2O_2 • Important application for diagnosis of diabetes mellitus	
Pt-NP loaded macrofiber	Chitin nanofiber	Reduction of *p*-nitrophenol	• Achieved strain value of about 12% • Work-of-fracture is around 10 MJ m^{-3} • Further loading with TiO_2 could enable photocatalytic property	141
Ag-NP/Au-NP/Pt-NP nanochitin aerogel	Nanofiber	Reduction of *p*-nitrophenol removing of organic dyes	• Highly stable • The approach can be extended to other metal nanoparticle catalysts	142
ZnO/chitin composite	Chitin/ZnO nanoparticle	Degrading NH_4^+-N under UV radiation	• 88.64% of NH_4^+-N removed in 2 h • Achieving catalyst cyclic utilization remains as unsolved problem	143
Cu_2O-chitin/graphene oxide (GO)	Nanocomposite	Methyl orange (MO) degradation under sunlight	• Nanochitin acts as a template for Cu_2O nanoparticle synthesis • GO dramatically improves the photocatalytic performance of Cu_2O *via* enhanced charge separation • Great potential for waste water treatment using solar energy	144
Chitin-derived carbon/ g-C_3N_4 heterojunction	Chitin-derived carbon nanoparticles	Rhodamine B degradation	• Non-metal photocatalyst is cost-effective and sustainable compared to metal based ones • Chitin creates microstructural change for g-C_3N_4, leading to an increase in surface area	145

(i) Its high surface area provides more active sites for loading metal catalysts and increases the accessibility of reactants to the catalyst.

(ii) Nanochitin is a biocompatible and biodegradable material, making it a sustainable and environmentally friendly alternative to synthetic support materials.

(iii) Nanochitin is highly chemically stable and can withstand harsh reaction conditions, making it a suitable support material for a wide range of metal catalysts.

(iv) Easy preparation: nanochitin can be easily prepared from natural chitin sources such as crustacean shells or fungal cell walls, making it a low-cost and readily available support material.

(v) Improved catalytic performance: nanochitin can improve the catalytic performance of metal catalysts due to its unique surface chemistry, which can enhance the adsorption of reactants and intermediates and increase the selectivity of the reaction.

The metal catalysts that can be supported by nanochitin include metal nanoparticles such as palladium, platinum, gold, and silver. Taking palladium nanoparticles (Pd NPs) as an example, nanochitin-supported Pd NPs have been used as catalysts for the Heck coupling reaction[139] and waste water treatment.[146] By directly reducing $PdCl_2$ salt in a one-pot fashion, Pd NPs were deposited on the chitin nanocrystals and formed hetero-structured catalysts.[139] The transmission electron microscopy images of the nanocomposites showed well-dispersed Pd NPs on the surface of the nanochitin crystals. The authors employed Heck coupling as the model reaction for testing the Pd NP-chitin catalyst, obtaining a full product yield under mild conditions, outperforming the use of other biomass-supported catalysts, such as cellulose nanocrystals.

Another highly efficient metal nanoparticle catalyst is platinum nanoparticles (Pt NPs), which are well known for their good catalytic performance in reactions such as hydrogenation, oxidation, and fuel cell reactions. Pt NPs exhibit high selectivity and stability even under harsh reaction conditions. However, Pt NPs easily aggregate, resulting in a reduction in the number of surface reactive sites when used alone. In this case, nanochitin is a great support substance for Pt NPs during the fabrication of the catalyst. Das *et al.* developed a recycled nanochitin hydrogel loaded with Pt NPs *via* the *in situ* reduction of H_2PtCl_6 salt in the hydrogel matrix.[141] These organic/inorganic hybrid hydrogel fibers showed high activity in the catalytic reduction of *p*-nitrophenol in the presence of $NaBH_4$. Moreover, these recyclable catalyst systems can be developed further with the addition of TiO_2 nanoparticles to perform photocatalytic reactions.

Silver nanoparticles (Ag NPs) are another type of multifunction nanoparticles, which are widely utilized in antibacterial coatings, sensors, water treatment, solar devices and catalytic reactions. As shown in Fig. 10a, with the dopamine-activated

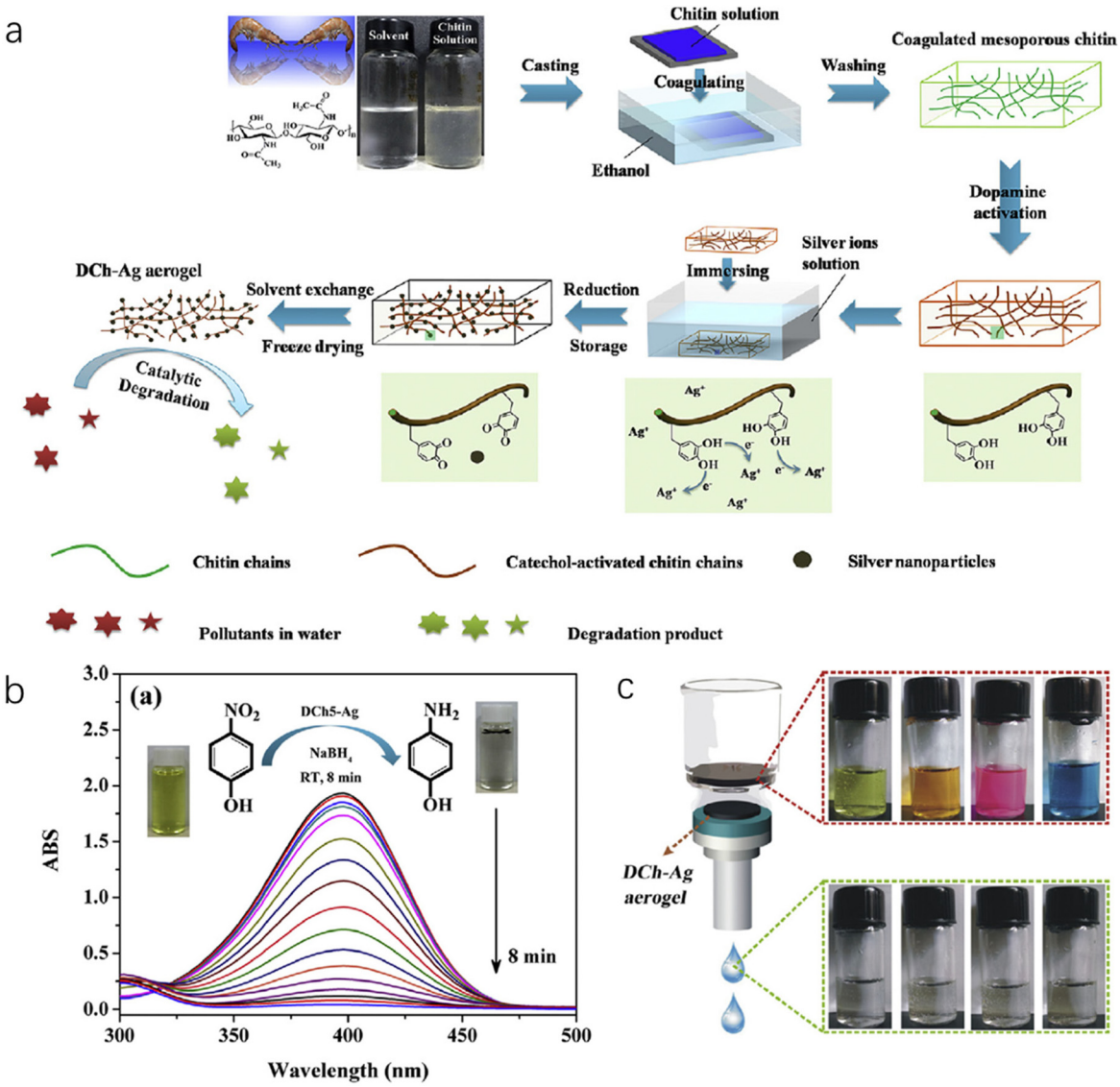

Fig. 10 (a) Illustration of the fabrication of the ChNC-Ag aerogel. (b) Catalytic evaluation of ChNC-Ag NP aerogels with a typical UV–vis spectra of the conversion reaction. The inset photographs show the color change from yellow (before) to colorless (after). (c) ChNC-Ag aerogels as filtration membranes to remove organic pollutants, where four colored organic dyes become colorless after the filtration process. Reproduced with permission.[142] Copyright 2017, Elsevier Inc.

nanochitin gel-like matrix, Ag^+ ions were introduced and further reduced into Ag NPs, followed by freeze drying to obtain an aerogel of hybrid Ag-nanochitin.[142] By controlling the activation of the nanochitin matrix *via* dopamine, the authors could control the storage capacity and the size distribution of metal nanoparticles precisely. Due to its high surface area, low density, tough mechanical strength and excellent catalytic activity, the hybrid aerogel reduced organic pollutants (such as methyl orange, methylene blue, *p*-nitrophenol and rhodamine B) in $NaBH_4$ medium, and examples are displayed in Fig. 10b and c, respectively. This approach can be used for generating many other catalytic metal nanoparticles with nanochitin aerogels, such as Au and Pt, as demonstrated by the authors in this work.

Finally, nanochitin can be chemically modified, for example, by introducing amino groups, chitin nanofibers can be used in filtration membranes, allowing the effective extraction of noble metal ions, such as Au^{3+}, Ag^+, Pt^{4+}, and Pd^{2+}.[140] As shown in the schematic drawing in Fig. 11a, firstly the nanochitin fiber membranes absorb metal ions from the oil/water emulsion, then upon the *in situ* reduction of the absorbed metal ions, metal nanoparticle-loaded nanochitin fibers were obtained.[140] Consequently, this nanochitin-supported metal catalyst is potentially useful for catalytic applications for biosensing and green catalyst production. Here, in this work, Au^{3+} was introduced to demonstrate the excellent catalytic property of the recovered Au NP-nanochitin fibers in the membrane form. The actual color of the recovered nano-

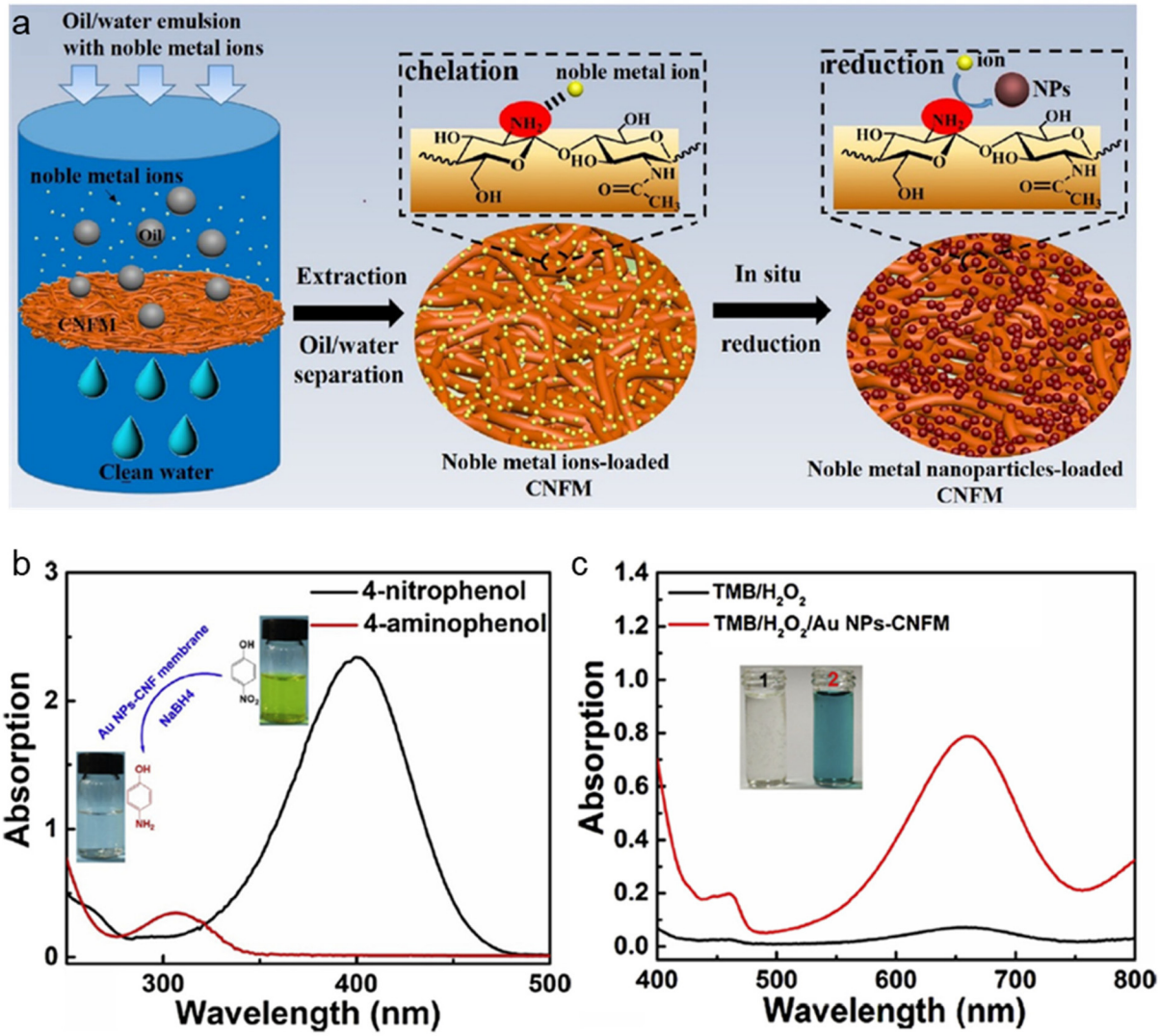

Fig. 11 (a) Scheme illustration of the recovery of noble metal ions from oil/water emulsions by chitin fibres membranes. (b) UV-vis of the 4-nitrophenolate/$NaBH_4$ before and after treatment using Au NP-nanochitin fibres. (c) UV–vis spectra of TMB/H_2O_2 before and after treatment by Au NP-nanochitin fibres. The insets are the photographs of TMB/H_2O_2 before (1) and after (2) treatment using Au NP-nanochitin fibres. Reproduced with permission.[140] Copyright 2019, Elsevier Ltd.

chitin membrane turned from yellow to red, and the TEM results demonstrated the appropriate size and crystallinity of the Au NPs. Two model reactions were chosen to test the Au NP-nanochitin fiber catalyst, with the results displayed in Fig. 11b and c, respectively. Employing the same approach, Ag, Pt and Pd nanoparticles could also be obtained for the metal nanoparticle-nanochitin fiber catalyst, although the authors did not report the details of this experiment. The successful recovery of the Au NP-chitin fiber membrane demonstrated its great catalytic activities and potential use in sensor and green catalysis systems.

Support or additive for inorganic photocatalysts. Metal oxides and other inorganic nanoparticles, such as titanium dioxide (TiO_2),[147,148] zinc oxide (ZnO),[143,149] copper oxide (Cu_2O)[144] and carbon nitride (C_3N_4),[145] can be deposited on the surface of nanochitin and used as a catalyst for various reactions. The biodegradability of nanochitin is advantageous, given that it reduces the environmental impact of catalyst synthesis and use. Some of the reported works are included in Table 3 for these materials, demonstrating their attractive properties and good photocatalytic behaviour.

Instead of deposition on the surface of nanochitin, Nguyen *et al.* utilized a different strategy known as liquid crystal self-assembly to develop TiO_2/graphene/chitin composite membranes.[150] Liquid crystals of both graphene oxide nanosheets and chitin nanospindles supposedly self-assembled into a flexible nacre-mimicking membrane and peroxotitanate were incorporated in the structure during the co-assembly process. A subsequent reduction was performed to produce TiO_2/graphene/chitin composite membranes. The absorption ability of

this composite membrane was revealed to be significantly enhanced compared to graphene oxide (~235 nm). In fact, the absorption range of the composite membrane was found to be extended to the visible light band (~450 nm). Additionally, they showed that the developed membrane could photo-catalyze methylene blue solution to colorless within 30 min of UV-Vis irradiation, which was faster than the controls (graphene and Degussa P25). This was attributed to the synergistic semiconductor-graphene interactions, which were possible by the heterojunction of the TiO_2 nanoparticle-localized graphene nanosheets supported onto nanochitin layers. Given that the surface chemistry of nanochitin can be modified to enhance its interaction with inorganic nanoparticles, together with the template effect, which facilitates the synthesis and distribution of the catalyst, nanochitin is an effective component that can improve the catalytic performance from several aspects.

4.4.2 Biocatalyst support. Biocatalysts are enzymes or microorganisms that can catalyze chemical reactions, which have a wide range of industrial and biomedical applications. Nanochitin has been used as a natural polymer support for various biocatalysts, including enzymes and whole cells.[151,152] The biodegradability of nanochitin is advantageous in biocatalytic applications given that it reduces the need for costly and environmentally harmful support material disposal. Additionally, the unique surface chemistry of nanochitin can be modified to enhance the interaction between the support material and biocatalysts, promoting improved biocatalyst stability and activity. To date, numerous biocatalysts have been reported, including lipase,[153,154] glucose oxidase mainly for biosensors,[155] and horseradish peroxidase.[156] The choice of immobilization method depends on the specific enzyme, choice of supporting materials and the intended application. Examples of the explored immobilization methods include physical adsorption, ionic binding and covalent binding.[157] Taking the enzymatic esterification reaction as one of the actual applications of lipase, a biocatalyst was developed *via* chitosan–chitin nanowhisker-supported *Rhizomucor miehei* lipase.[158] Under the optimized conditions, the authors reported a maximum yield of 66% at 50 °C in a 5 h reaction. Furthermore, the immobilized lipase as an efficient biocatalyst could be used for up to 8 cycles of esterification without degradation.

Nanochitin serves as immobilization support for enzymes and other biocatalysts and is very useful in industrial biotechnology such as the production of pharmaceuticals, food processing, and biofuels. In general, the immobilization of enzymes on nanochitin can improve their stability, activity, and reusability, leading to more efficient and cost-effective enzyme-catalyzed processes.

4.4.3 Organocatalyst. Organocatalysis is a type of catalysis that involves the use of organic molecules as catalysts to promote chemical reactions. Nanochitin has been shown to have catalytic activity in various organic reactions, such as Michael addition, aldol reaction, hydrolysis of cellulose and synthesis of organic carbonates. As a biopolymer organocatalyst, nanochitin is more advantageous than the traditional organic molecules due to the following reasons:

(i) The high surface area of nanochitin allows for a greater number of active sites, leading to higher catalytic activity.

(ii) The biocompatibility of nanochitin also makes it a more sustainable and environmentally friendly alternative to synthetic organic catalysts.

(iii) Given that the amino and carboxyl functional groups in nanochitin can participate in the reaction mechanism, it can be more selective and achieve higher catalytic efficiency.

Tsutsumi *et al.* reported the synthesis of a highly porous nanochitin aerogel with C2-amine-functionalized chitin nanofibrils (ChNF), exhibiting high surface areas.[159] The obtained nanochitin aerogel was employed as a catalyst for the aqueous Knoevenagel condensation reaction, achieving high efficiency due to the combination of active amine groups and the nanofibrous structure supporting continuous flow catalysis. Amino-functionalized nanochitin and chitosan have been shown to be an effective catalyst for the solvent-free synthesis of chalcones,[160] self-condensation of linear aldehydes[161] and production of biodiesel.[162] Nanochitin can also be used as a bioreactor for various purposes, such as sulfate reducing for mining influenced water,[163] metal removal and acid neutralization,[164] as well as creating a multienzyme bioreactor.[165] The high surface area of nanochitin allows for efficient cell attachment and growth, and its unique surface chemistry can be modified to enhance the interaction between cells and the supporting material.

However, although nanochitin has great potential for use in catalytic applications due to its unique properties and versatility, further research is needed to fully understand its catalytic activity and optimize its use in different applications.

In summary, the use of natural polysaccharides such as chitin as either a catalyst support or organocatalyst is an emerging trend in green and sustainable chemistry. However, there is still exciting scope that remains unexplored in utilizing natural polymers in sustainable chemistry. For instance, they can be explored as catalysts for the oxygen evolution reaction[166,167] and high-kinetics oxygen reduction reaction.[168]

5 Conclusion and perspective

In this review, we summarized the different strategies to prepare nanochitin from chitin. We examined these strategies from a different viewpoint by identifying the comparably more sustainable methods from the traditional methods. For instance, researchers have explored the use of greener solvents and ways to optimize the process to be more environmentally friendly. It is recognized that chitin sources can be obtained from various biomass such as crustaceans, insects, and fungi. However, the efficiency of chitin isolation from these sources is different, even when the same technique is used due to the different compositions that it is found in. For example, chitin extraction from insect exoskeleton is likely to be easier than chitin isolation from crustacean shells, where the mineral

content is higher. Not only can milder conditions be used for the former, but the yield can also be higher.

At present, the chitin biorefinery is not as established as its cellulose counterpart. With reference to the market size of nanocellulose, it can be safely estimated that there will be a market for nanochitin. In fact, the market size of nanochitin will not be small and likely to be even bigger than nanocellulose. The reason for this is that nanochitin is the only natural polysaccharide that contains nitrogen. Although the actual extent of demand for nanochitin and its products is still unclear, all the above-mentioned studies demonstrated that nanochitin will be valuable as a sustainable and advanced materials for future manufacturing, consumer care, and even biomedicine.

It seems that several challenges need to be overcome in the process of establishing the chitin biorefinery. The first challenge is to isolate and obtain homogeneous sources of biomass waste. There is also the problem with resource complexity, whereby different sources have different chitin contents. Furthermore, currently, the nanochitin extraction methods are still not very eco-friendly with low yield, despite being energy intensive. The characterization, processing and modification methods are very limited at this stage. At present, nanochitin is mostly applied as an additive instead of bulk material and more studies will be needed to understand its interaction with the host matrix. There is also the question of the feasibility of scale up, which should be possible given that its predecessor is nanocellulose. However, the success of scaling up eventually depends on the techniques employed to extract chitin and convert it to nanochitin as well as the efficiency. A crucial and unavoidable issue will be the cost of nanochitin fabrication given that a high cost will deter its use for applications.

Besides the challenges encountered in the set-up of the chitin biorefinery, it is necessary to consider the environmental impact of the nanochitin fabrication from cradle to grave. It is important to reduce and valorize waste; however, there should not be more waste generated in the process of doing so. Thus, life cycle assessments will be a powerful tool to gauge the "real" environmental benefits of nanochitin synthesis from biomass waste.

Finally, the potential applications for nanochitin in advanced manufacturing that have been explored by researchers were presented, which range from 3D printing and photonics to packaging and catalysis. Indeed, nanochitin appears to have numerous advantages that can be imparted to the materials. However, in most cases nanochitin can only be used as additives or supportive materials. Thus, how to better explore its advantage and maximize its potential is something worthy to investigate to achieve a circular economy.

Conflicts of interest

The authors declare no conflict of interest.

Acknowledgements

This research is supported by the RIE2025 MTC Individual Research Grants (M22K2c0085) and Urban and Green Technology Horizontal Technology Seed Fund (C211718009), administered by the Agency of Science, Technology and Research (A*STAR), Singapore. This work was also supported by the National Medical Research Council (NMRC), Singapore, under its Clinician Scientist-Individual Research Grant (MOH-001357-00).

References

1 L. Bai, L. Liu, M. Esquivel, B. L. Tardy, S. Huan, X. Niu, S. Liu, G. Yang, Y. Fan and O. J. Rojas, *Chem. Rev.*, 2022, **122**, 11604–11674.
2 H.-S. Jung, H. C. Kim and W. H. Park, *Carbohydr. Polym.*, 2019, **213**, 311–319.
3 S. Olza, A. M. Salaberria, A. Alonso-Varona, A. Samanta and S. C. M. Fernandes, *J. Mater. Chem. B*, 2023, **11**, 5630–5649.
4 T. Jin, T. Liu, E. Lam and A. Moores, *Nanoscale Horiz.*, 2021, **6**, 505–542.
5 H. Ma, L. Liu, J. Yu and Y. Fan, *Biomacromolecules*, 2021, **22**, 4373–4382.
6 X. Ma, G. Gözaydın, H. Yang, W. Ning, X. Han, N. Y. Poon, H. Liang, N. Yan and K. Zhou, *Proc. Natl. Acad. Sci. U. S. A.*, 2020, **117**, 7719–7728.
7 I. Younes and M. Rinaudo, *Mar. Drugs*, 2015, **13**, 1133–1174.
8 B. T. Iber, N. A. Kasan, D. Torsabo and J. W. Omuwa, *J. Renewable Mater.*, 2022, **10**, 1097–1123.
9 X. Yang, J. Liu, Y. Pei, X. Zheng and K. Tang, *Energy Environ. Mater.*, 2020, **3**, 492–515.
10 E. Alabaraoye, M. Achilonu and R. Hester, *J. Polym. Environ.*, 2017, **26**, 2207–2218.
11 C. Peniche, W. Argüelles-Monal and F. M. Goycoolea, in *Monomers, Polymers and Composites from Renewable Resources*, ed. M. N. Belgacem and A. Gandini, Elsevier, Amsterdam, 2008, pp. 517–542, DOI: 10.1016/B978-0-08-045316-3.00025-9.
12 K. Mohan, T. Muralisankar, R. Jayakumar and C. Rajeevgandhi, *Carbohydr. Polym. Technol. Appl.*, 2021, **2**, DOI: 10.1016/j.carpta.2021.100037.
13 A. van Huis, *J. Insects Food Feed*, 2020, **6**, 27–44.
14 G. Huet, C. Hadad, E. Husson, S. Laclef, V. Lambertyn, M. A. Farias, A. Jamali, M. Courty, R. Alayoubi, I. Gosselin, C. Sarazin and A. N. Van Nhien, *Carbohydr. Polym.*, 2020, **228**, 115382.
15 L. Soetemans, M. Uyttebroek and L. Bastiaens, *Int. J. Biol. Macromol.*, 2020, **165**, 3206–3214.
16 R. Chandran, L. Williams, A. Hung, K. Nowlin and D. LaJeunesse, *Micron*, 2016, **82**, 74–85.
17 K. P. Sambasevam, S. F. Sateria, S. N. A. Baharin, N. J. Azman, S. A. Wakid and S. Shahabuddin, *Int. J. Biol. Macromol.*, 2023, **238**, 124079.
18 M. Jones, M. Kujundzic, S. John and A. Bismarck, *Mar. Drugs*, 2020, **18**, 64.

19 J. Sietsma and J. Wessels, *Biochim. Biophys. Acta, Gen. Subj.*, 1977, **496**, 225–239.
20 J. Vetter, *Food Chem.*, 2007, **102**, 6–9.
21 Y. Bamba, Y. Ogawa, T. Saito, L. A. Berglund and A. Isogai, *Biomacromolecules*, 2017, **18**, 4405–4410.
22 C. M. Stagg and M. S. Feather, *Biochim. Biophys. Acta, Gen. Subj.*, 1973, **320**, 64–72.
23 A. M. Salaberria, J. Labidi and S. C. Fernandes, *Eur. Polym. J.*, 2015, **68**, 503–515.
24 R. N. Tharanathan and F. S. Kittur, *Crit. Rev. Food Sci. Nutr.*, 2003, **43**, 61–87.
25 J. D. Goodrich and W. T. Winter, *Biomacromolecules*, 2007, **8**, 252–257.
26 S. Ling, D. L. Kaplan and M. J. Buehler, *Nat. Rev. Mater.*, 2018, **3**, 1–15.
27 H. O. Fabritius, C. Sachs, P. R. Triguero and D. Raabe, *Adv. Mater.*, 2009, **21**, 391–400.
28 R. Marchessault, F. Morehead and N. Walter, *Nature*, 1959, **184**, 632–633.
29 J.-F. Revol and R. Marchessault, *Int. J. Biol. Macromol.*, 1993, **15**, 329–335.
30 K. Kurita, K. Tomita, T. Tada, S. Ishii, S. I. Nishimura and K. Shimoda, *J. Polym. Sci., Part A: Polym. Chem.*, 1993, **31**, 485–491.
31 A. Morin and A. Dufresne, *Macromolecules*, 2002, **35**, 2190–2199.
32 K. Gopalan Nair and A. Dufresne, *Biomacromolecules*, 2003, **4**, 657–665.
33 K. Gopalan Nair, A. Dufresne, A. Gandini and M. N. Belgacem, *Biomacromolecules*, 2003, **4**, 1835–1842.
34 J. Sriupayo, P. Supaphol, J. Blackwell and R. Rujiravanit, *Carbohydr. Polym.*, 2005, **62**, 130–136.
35 P. Wongpanit, N. Sanchavanakit, P. Pavasant, T. Bunaprasert, Y. Tabata and R. Rujiravanit, *Eur. Polym. J.*, 2007, **43**, 4123–4135.
36 Z. Li, H. Wang, S. An and X. Yin, *J. Nanobiotechnol.*, 2021, **19**, 1–13.
37 Y. Zhou, S. Jiang, Y. Jiao and H. Wang, *Int. J. Biol. Macromol.*, 2017, **99**, 205–212.
38 Y. Qin, S. Zhang, J. Yu, J. Yang, L. Xiong and Q. Sun, *Carbohydr. Polym.*, 2016, **147**, 372–378.
39 Y. F. Aklog, M. Egusa, H. Kaminaka, H. Izawa, M. Morimoto, H. Saimoto and S. Ifuku, *Int. J. Mol. Sci.*, 2016, **17**, 1600.
40 Y. F. Aklog, T. Nagae, H. Izawa, M. Morimoto, H. Saimoto and S. Ifuku, *J. Nanosci. Nanotechnol.*, 2017, **17**, 5037–5041.
41 P.-Y. Chen, A. Y.-M. Lin, J. McKittrick and M. A. Meyers, *Acta Biomater.*, 2008, **4**, 587–596.
42 K. Missoum, M. N. Belgacem and J. Bras, *Materials*, 2013, **6**, 1745–1766.
43 S. Ifuku, M. Nogi, K. Abe, M. Yoshioka, M. Morimoto, H. Saimoto and H. Yano, *Carbohydr. Polym.*, 2011, **84**, 762–764.
44 S. Ifuku, M. Nogi, M. Yoshioka, M. Morimoto, H. Yano and H. Saimoto, *Carbohydr. Polym.*, 2010, **81**, 134–139.
45 J. H. Bang and K. S. Suslick, *Adv. Mater.*, 2010, **22**, 1039–1059.
46 M. N. Islam, M. Zhang and B. Adhikari, *Food Rev. Int.*, 2014, **30**, 1–21.
47 Y. Lu, Q. Sun, X. She, Y. Xia, Y. Liu, J. Li and D. Yang, *Carbohydr. Polym.*, 2013, **98**, 1497–1504.
48 Y. Fan, T. Saito and A. Isogai, *Biomacromolecules*, 2008, **9**, 192–198.
49 S. Ifuku, T. Hori, H. Izawa, M. Morimoto and H. Saimoto, *Carbohydr. Polym.*, 2015, **122**, 1–4.
50 Y. Fan, T. Saito and A. Isogai, *Carbohydr. Polym.*, 2009, **77**, 832–838.
51 K. Pang, B. Ding, X. Liu, H. Wu, Y. Duan and J. Zhang, *Green Chem.*, 2017, **19**, 3665–3670.
52 J. Jiang, J. Yu, L. Liu, Z. Wang, Y. Fan and A. Isogai, *J. Agric. Food Chem.*, 2018, **66**, 11372–11379.
53 Y. Fan, T. Saito and A. Isogai, *Carbohydr. Polym.*, 2010, **79**, 1046–1051.
54 E. Belamie, P. Davidson and M. Giraud-Guille, *J. Phys. Chem. B*, 2004, **108**, 14991–15000.
55 J. Xu, X. Deng, Y. Dong, Z. Zhou, Y. Zhang, J. Yu, J. Cai and Y. Zhang, *Carbohydr. Polym.*, 2020, **247**, 116694.
56 R. Nayak, R. Padhye, I. L. Kyratzis, Y. B. Truong and L. Arnold, *Text. Res. J.*, 2012, **82**, 129–147.
57 P. S. Barber, C. S. Griggs, J. R. Bonner and R. D. Rogers, *Green Chem.*, 2013, **15**, 601–607.
58 T. Kida, S.-I. Sato, H. Yoshida, A. Teragaki and M. Akashi, *Chem. Commun.*, 2014, **50**, 14245–14248.
59 R. M. Street, *Electrospun Scaffolds for Spinal Cord Explant Cultures*, Drexel University, 2018.
60 B.-M. Min, S. W. Lee, J. N. Lim, Y. You, T. S. Lee, P. H. Kang and W. H. Park, *Polymer*, 2004, **45**, 7137–7142.
61 Y. Huang, Z. Zhong, B. Duan, L. Zhang, Z. Yang, Y. Wang and Q. Ye, *J. Mater. Chem. B*, 2014, **2**, 3427–3432.
62 K. Zhu, H. Tu, P. Yang, C. Qiu, D. Zhang, A. Lu, L. Luo, F. Chen, X. Liu and L. Chen, *Chem. Mater.*, 2019, **31**, 2078–2087.
63 H. Wu, G. R. Williams, J. Wu, J. Wu, S. Niu, H. Li, H. Wang and L. Zhu, *Carbohydr. Polym.*, 2018, **180**, 304–313.
64 C. Zhong, A. Cooper, A. Kapetanovic, Z. Fang, M. Zhang and M. Rolandi, *Soft Matter*, 2010, **6**, 5298–5301.
65 M. Rolandi and R. Rolandi, *Adv. Colloid Interface Sci.*, 2014, **207**, 216–222.
66 B. Duan, Y. Huang, A. Lu and L. Zhang, *Prog. Polym. Sci.*, 2018, **82**, 1–33.
67 M. A. Surati, S. Jauhari and K. Desai, *Arch. Appl. Sci. Res.*, 2012, **4**, 645–661.
68 R. Fernández-Marín, F. Hernández-Ramos, A. M. Salaberria, M. Á. Andrés, J. Labidi and S. C. Fernandes, *Int. J. Biol. Macromol.*, 2021, **186**, 218–226.
69 C. M. Keck and R. H. Müller, *Eur. J. Pharm. Biopharm.*, 2006, **62**, 3–16.
70 A. M. Salaberria, S. C. Fernandes, R. H. Diaz and J. Labidi, *Carbohydr. Polym.*, 2015, **116**, 286–291.
71 W. Ye, S. Yokota, Y. Fan and T. Kondo, *Cellulose*, 2021, **28**, 2167–2181.

72 R. Kose and T. Kondo, *Sen'i Gakkaishi*, 2011, **67**, 91–95.
73 K. Ishida, S. Yokota and T. Kondo, *J. Fiber Sci. Technol.*, 2021, **77**, 203–212.
74 S. Ifuku, K. Yamada, M. Morimoto and H. Saimoto, *J. Nanomater.*, 2012, **2012**, DOI: 10.1155/2012/645624.
75 S. Ifuku, K. Yamada, M. Morimoto and H. Saimoto, *J. Nanomater.*, 2012, **2012**, 645624.
76 G. A. Baker, S. N. Baker, S. Pandey and F. V. Bright, *Analyst*, 2005, **130**, 800–808.
77 J.-I. Kadokawa, A. Takegawa, S. Mine and K. Prasad, *Carbohydr. Polym.*, 2011, **84**, 1408–1412.
78 E. L. Smith, A. P. Abbott and K. S. Ryder, *Chem. Rev.*, 2014, **114**, 11060–11082.
79 M. Sharma, C. Mukesh, D. Mondal and K. Prasad, *RSC Adv.*, 2013, **3**, 18149–18155.
80 C. Mukesh, D. Mondal, M. Sharma and K. Prasad, *Carbohydr. Polym.*, 2014, **103**, 466–471.
81 Y. Yuan, S. Hong, H. Lian, K. Zhang and H. Liimatainen, *Carbohydr. Polym.*, 2020, **236**, 116095.
82 S. Hong, Y. Yuan, Q. Yang, L. Chen, J. Deng, W. Chen, H. Lian, J. D. Mota-Morales and H. Liimatainen, *Carbohydr. Polym.*, 2019, **220**, 211–218.
83 S. Hong, Y. Yuan, K. Zhang, H. Lian and H. Liimatainen, *Nanomaterials*, 2020, **10**, 869.
84 L. Barandiaran, B. Alonso-Lerma, A. Reifs, I. Larraza, R. Olmos-Juste, A. Fernandez-Calvo, Y. Jabalera, A. Eceiza and R. Perez-Jimenez, *Commun. Mater.*, 2022, **3**, 55.
85 J. Lv, Y. Zhang, Y. Jin, D.-H. Oh and X. Fu, *Int. J. Biol. Macromol.*, 2024, **254**, 127662.
86 A. M. Salaberria, R. H. Diaz, J. Labidi and S. C. Fernandes, *Food Hydrocolloids*, 2015, **46**, 93–102.
87 S. Shankar, J. P. Reddy, J.-W. Rhim and H.-Y. Kim, *Carbohydr. Polym.*, 2015, **117**, 468–475.
88 H.-S. Jung, M. H. Kim and W. H. Park, *ACS Biomater. Sci. Eng.*, 2019, **5**, 1744–1752.
89 C. Zhang, X. Zhuang, X. Li, W. Wang, B. Cheng, W. Kang, Z. Cai and M. Li, *Carbohydr. Polym.*, 2016, **140**, 195–201.
90 H. K. Noh, S. W. Lee, J.-M. Kim, J.-E. Oh, K.-H. Kim, C.-P. Chung, S.-C. Choi, W. H. Park and B.-M. Min, *Biomaterials*, 2006, **27**, 3934–3944.
91 H. Zou, B. Lin, C. Xu, M. Lin and W. Zhan, *Cellulose*, 2018, **25**, 999–1010.
92 Y. Qin, X. Lu, N. Sun and R. D. Rogers, *Green Chem.*, 2010, **12**, 968–971.
93 N. Yang, W. Zhang, C. Ye, X. Chen and S. Ling, *Biotechnol. J.*, 2019, **14**, e1700754.
94 I. Muñoz, C. Rodríguez, D. Gillet and B. M. Moerschbacher, *Int. J. Life Cycle Assess.*, 2017, **23**, 1151–1160.
95 P. Cinelli, M. Coltelli, N. Mallegni, P. Morganti and A. Lazzeri, *Chem. Eng. Trans.*, 2017, **60**, 115–120.
96 P. S. Gungor-Ozkerim, I. Inci, Y. S. Zhang, A. Khademhosseini and M. R. Dokmeci, *Biomater. Sci.*, 2018, **6**, 915–946.
97 X. Cui, J. Li, Y. Hartanto, M. Durham, J. Tang, H. Zhang, G. Hooper, K. Lim and T. Woodfield, *Adv. Healthcare Mater.*, 2020, **9**, 1901648.
98 Y. Zhang, D. Zhou, J. Chen, X. Zhang, X. Li, W. Zhao and T. Xu, *Mar. Drugs*, 2019, **17**, 555.
99 B. Mahendiran, S. Muthusamy, S. Sampath, S. Jaisankar, K. C. Popat, R. Selvakumar and G. S. Krishnakumar, *Int. J. Biol. Macromol.*, 2021, **183**, 564–588.
100 P. Karimipour-Fard, M. P. Jeffrey, H. JonesTaggart, R. Pop-Iliev and G. Rizvi, *J. Mech. Behav. Biomed. Mater.*, 2021, **120**, 104583.
101 B. Sadhasivam, D. Ramamoorthy and R. Dhamodharan, *Int. J. Biol. Macromol.*, 2020, **165**, 3145–3155.
102 Z. Ling, J. Zhao, S. Song, S. Xiao, P. Wang, Z. An, Z. Fu, J. Shao, Z. Zhang, W. Fu and S. Song, *Regener. Biomater.*, 2023, **10**, rbad058.
103 R. Zhang, L. Deng, J. Guo, H. Yang, L. Zhang, X. Cao, A. Yu and B. Duan, *ACS Nano*, 2021, **15**, 17790–17803.
104 E. Lizundia, T.-D. Nguyen, R. J. Winnick and M. J. MacLachlan, *J. Mater. Chem. C*, 2021, **9**, 796–817.
105 Y. Zhao, Z. Xie, H. Gu, C. Zhu and Z. Gu, *Chem. Soc. Rev.*, 2012, **41**, 3297–3317.
106 J. Hou, B. E. Aydemir and A. G. Dumanli, *Philos. Trans. R. Soc., A*, 2021, **379**, 20200331.
107 R. Boruah, P. Nath, D. Mohanta, G. A. Ahmed and A. Choudhury, *Nanosci. Nanotechnol. Lett.*, 2011, **3**, 458–462.
108 Z. Mu, X. Zhao, Z. Xie, Y. Zhao, Q. Zhong, L. Bo and Z. Gu, *J. Mater. Chem. B*, 2013, **1**, 1607–1613.
109 J. Tian, W. Zhang, J. Gu, T. Deng and D. Zhang, *Nano Energy*, 2015, **17**, 52–62.
110 S. Wei, Y. Li, K. Li, A. Kang, S. Zhang, T. Feng, H. Zhang and C. Zhong, *Mater. Today Bio*, 2022, **13**, 100179.
111 P. Liu, J. Wang, H. Qi, T. Koddenberg, D. Xu, S. Liu and K. Zhang, *Nano Today*, 2022, **43**, DOI: 10.1016/j.nantod.2022.101420.
112 T.-D. Nguyen and M. J. MacLachlan, *Adv. Opt. Mater.*, 2019, **7**, 1801275.
113 C. P. Barrera-Patiño, J. D. Vollet-Filho, R. G. Teixeira-Rosa, H. P. Quiroz, A. Dussan, N. M. Inada, V. S. Bagnato and R. R. Rey-González, *Sci. Rep.*, 2020, **10**, 5786.
114 A. Narkevicius, R. M. Parker, J. Ferrer-Orri, T. G. Parton, Z. Lu, G. T. van de Kerkhof, B. Frka-Petesic and S. Vignolini, *Adv. Mater.*, 2022, **34**, 2203300.
115 T. Changcharoen, T. Apiphatnaphakul, W. Watjanavarreerat and K. Locharoenrat, *Artif. Cells, Nanomed., Biotechnol.*, 2022, **50**, 87–95.
116 T. D. Nguyen, K. E. Shopsowitz and M. J. MacLachlan, *Chemistry*, 2013, **19**, 15148–15154.
117 T.-D. Nguyen and M. J. MacLachlan, *Adv. Opt. Mater.*, 2014, **2**, 1031–1037.
118 C. Mille, E. C. Tyrode and R. W. Corkery, *RSC Adv.*, 2013, **3**, 3109–3117.
119 I. Zada, W. Zhang, Y. Li, P. Sun, N. Cai, J. Gu, Q. Liu, H. Su and D. Zhang, *Appl. Phys. Lett.*, 2016, **109**, DOI: 10.1063/1.4962903.
120 S. Ngasotter, L. Sampath and K. A. M. Xavier, *Carbohydr. Polym.*, 2022, **291**, 119627.
121 B. Yousuf, K. Gul, A. A. Wani and P. Singh, *Crit. Rev. Food Sci. Nutr.*, 2016, **56**, 2223–2230.

122 N. Bhargava, V. S. Sharanagat, R. S. Mor and K. Kumar, *Trends Food Sci. Technol.*, 2020, **105**, 385–401.
123 Y. Zheng, X. Li, Y. Huang, H. Li, L. Chen and X. Liu, *Food Hydrocolloids*, 2022, **127**, DOI: **10.1016/j.foodhyd.2022.107517**.
124 M. Chen, T. Yan, J. Huang, Y. Zhou and Y. Hu, *Int. J. Biol. Macromol.*, 2021, **179**, 90–100.
125 M. A. Sani, M. Tavassoli, H. Hamishehkar and D. J. McClements, *Carbohydr. Polym.*, 2021, **255**, 117488.
126 Y.-N. Yang, K.-Y. Lu, P. Wang, Y.-C. Ho, M.-L. Tsai and F.-L. Mi, *Carbohydr. Polym.*, 2020, **228**, 115370.
127 G. Cabrera-Barjas, N. Radovanovic, G. B. Arrepol, A. F. de la Torre, O. Valdes and A. Nesic, *Int. J. Biol. Macromol.*, 2021, **186**, 92–99.
128 R. Fernández-Marín, S. C. M. Fernandes, M. Á. A. Sánchez and J. Labidi, *Food Hydrocolloids*, 2022, **123**, DOI: **10.1016/j.foodhyd.2021.107119**.
129 M. Duan, S. Yu, J. Sun, H. Jiang, J. Zhao, C. Tong, Y. Hu, J. Pang and C. Wu, *Int. J. Biol. Macromol.*, 2021, **187**, 332–340.
130 C. Wu, H. Jiang, J. Zhao, M. Humayun, S. Wu, C. Wang, Z. Zhi and J. Pang, *Food Hydrocolloids*, 2022, **133**, DOI: **10.1016/j.foodhyd.2022.107998**.
131 S. Lee, L. T. Hao, J. Park, D. X. Oh and D. S. Hwang, *Adv. Mater.*, 2023, **35**, 2203325.
132 S. Ngasotter, L. Sampath and K. M. Xavier, *Carbohydr. Polym.*, 2022, 119627.
133 F. A. Yihun, *Emergent Mater.*, 2022, 1–30.
134 T. Jin, T. Liu, E. Lam and A. Moores, *Nanoscale Horiz.*, 2021, **6**, 505–542.
135 V. G. Matveeva and L. M. Bronstein, *Prog. Mater. Sci.*, 2022, 100999.
136 M. Dohendou, K. Pakzad, Z. Nezafat, M. Nasrollahzadeh and M. G. Dekamin, *Int. J. Biol. Macromol.*, 2021, **192**, 771–819.
137 N. Reddy, Y. Yang, N. Reddy and Y. Yang, *Innovative Biofibers from Renewable Resources*, 2015, pp. 449–450.
138 P. T. A. Le, T. P. Vu, H. T. Le, D. Van Phan, C. X. Nguyen, T. D. Luong, N. T. T. Dang and T. D. Nguyen, *J. Electron. Mater.*, 2020, **49**, 3791–3803.
139 T. Jin, M. Hicks, D. Kurdyla, S. Hrapovic, E. Lam and A. Moores, *Beilstein J. Org. Chem.*, 2020, **16**, 2477–2483.
140 Z. Wang, P. Li, Y. Fang, L. Yan, W. Zhou, X. Fan and H. Liu, *Carbohydr. Polym.*, 2019, **223**, 115064.
141 P. Das, T. Heuser, A. Wolf, B. Zhu, D. E. Demco, S. Ifuku and A. Walther, *Biomacromolecules*, 2012, **13**, 4205–4212.
142 Y. Wang, Q. Kong, B. Ding, Y. Chen, X. Yan, S. Wang, F. Chen, J. You and C. Li, *J. Colloid Interface Sci.*, 2017, **505**, 220–229.
143 X. Lin, A. Yang, G. Huang, X. Zhou, Y. Zhai, X. Chen and E. McBean, *Water*, 2019, **11**, DOI: **10.3390/w11020310**.
144 Y. Wang, Y. Pei, W. Xiong, T. Liu, J. Li, S. Liu and B. Li, *Int. J. Biol. Macromol.*, 2015, **81**, 477–482.
145 B. He, M. Feng, X. Chen, D. Zhao and J. Sun, *Appl. Surf. Sci.*, 2020, **527**, DOI: **10.1016/j.apsusc.2020.146737**.
146 W. Wang, M. N. Nadagouda and S. M. Mukhopadhyay, *Nanomaterials*, 2022, **12**, 3593.
147 K. Mao, X. Wu, X. Min, Z. Huang, Y. G. Liu and M. Fang, *Sci. Rep.*, 2019, **9**, 16321.
148 S. Khaoulani, H. Chaker, C. Cadet, E. Bychkov, L. Cherif, A. Bengueddach and S. Fourmentin, *C. R. Chim.*, 2015, **18**, 23–31.
149 X. Di, F. Guo, Z. Zhu, Z. Xu, Z. Qian and Q. Zhang, *RSC Adv.*, 2019, **9**, 41209–41217.
150 P. T. A. Le, T. P. Vu, H. T. Le, D. Van Phan, C. X. Nguyen, T. D. Luong, N. T. T. Dang and T. D. Nguyen, *J. Electron. Mater.*, 2020, **49**, 3791–3803.
151 B. Thangaraj and P. R. Solomon, *ChemBioEng Rev.*, 2019, **6**, 167–194.
152 M. L. Verma, S. Kumar, A. Das, J. S. Randhawa and M. Chamundeeswari, *Environ. Chem. Lett.*, 2020, **18**, 315–323.
153 B. R. Facin, M. S. Melchiors, A. Valério, J. V. Oliveira and D. d. Oliveira, *Ind. Eng. Chem. Res.*, 2019, **58**, 5358–5378.
154 M. Bilal, C. D. Fernandes, T. Mehmood, F. Nadeem, Q. Tabassam and L. F. R. Ferreira, *Int. J. Biol. Macromol.*, 2021, **175**, 108–122.
155 W. Suginta, P. Khunkaewla and A. Schulte, *Chem. Rev.*, 2013, **113**, 5458–5479.
156 T. Machałowski, K. Jankowska, K. Bachosz, W. Smułek, H. Ehrlich, E. Kaczorek, J. Zdarta and T. Jesionowski, *Molecules*, 2022, **27**, 1354.
157 W. A. Mehdi, A. A. Mehde, M. Ozacar and Z. Ozacar, *Int. J. Biol. Macromol.*, 2018, **117**, 947–958.
158 F. M. A. Manan, N. Attan, Z. Zakaria, A. S. A. Keyon and R. A. Wahab, *Enzyme Microb. Technol.*, 2018, **108**, 42–52.
159 Y. Tsutsumi, H. Koga, Z. D. Qi, T. Saito and A. Isogai, *Biomacromolecules*, 2014, **15**, 4314–4319.
160 Hernawan, B. Purwono, Triyono and M. Hanafi, *J. Taiwan Inst. Chem. Eng.*, 2022, **134**, DOI: **10.1016/j.jtice.2022.104354**.
161 T. Jose, N. Sudheesh and R. S. Shukla, *J. Mol. Catal. A: Chem.*, 2010, **333**, 158–166.
162 B. Aghabarari, *J. Renewable Energy Environ.*, 2016, **3**, 57–62.
163 S. R. Al-Abed, P. X. Pinto, J. McKernan, E. Feld-Cook and S. M. Lomnicki, *Chem. Eng. J.*, 2017, **323**, 270–277.
164 Z. DiLoreto, P. Weber, W. Olds, J. Pope, D. Trumm, S. Chaganti, D. Heath and C. Weisener, *J. Environ. Manage.*, 2016, **183**, 601–612.
165 E. Vlakh, E. Ponomareva and T. Tennikova, *Appl. Biochem. Microbiol.*, 2014, **50**, 441–446.
166 D. Yu, Y. Hao, S. Han, S. Zhao, Q. Zhou, C.-H. Kuo, F. Hu, L. Li, H.-Y. Chen, J. Ren and S. Peng, *ACS Nano*, 2023, **17**, 1701–1712.
167 Y. Hao, S.-F. Hung, W.-J. Zeng, Y. Wang, C. Zhang, C.-H. Kuo, L. Wang, S. Zhao, Y. Zhang, H.-Y. Chen and S. Peng, *J. Am. Chem. Soc.*, 2023, **145**, 23659–23669.
168 H. Huang, A. Huang, D. Liu, W. Han, C.-H. Kuo, H.-Y. Chen, L. Li, H. Pan and S. Peng, *Adv. Mater.*, 2023, **35**, 2303109.